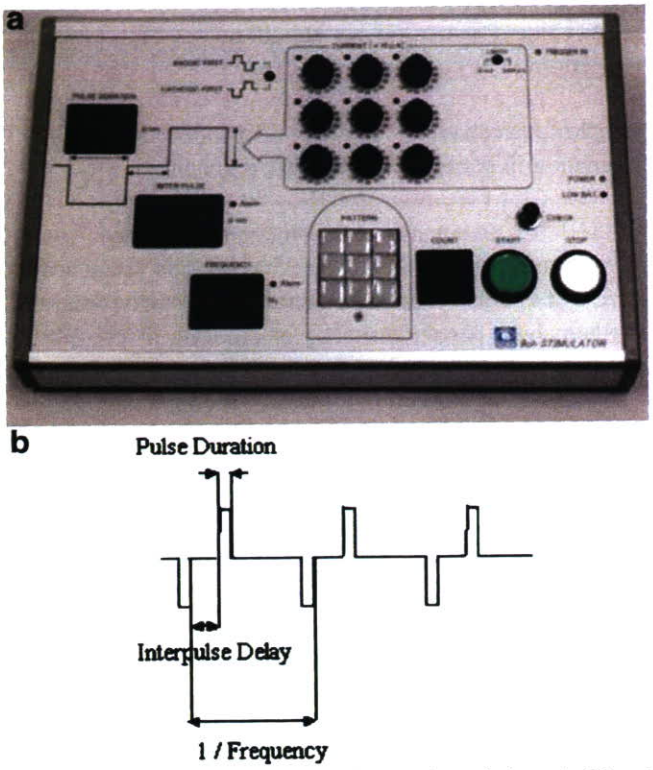

Fig. 3 Photograph of the stimulator for a 9-channel electrode (**a**) and the diagram of stimulating current pulse (**b**). **a** Charge-balanced biphasic pulses were delivered to individual electrodes simultaneously. **b** The first pulse delivers a cathodic current while the second pulse delivers anodic current to balance the charge

identify the threshold current. Care was taken not to influence the description by the patients.

After determining the threshold current of each electrode, simultaneous multi-channel stimulation was performed to examine if patients could achieve two-point discrimination or pattern recognition.

Statistical analyses

Data are presented as the means ± standard error of the means (SEM) and were statistically analyzed with the SPSS 10.0J program (SPSS Inc, Chicago, IL). Comparisons between two groups were made by the Student's *t* test when data were normally distributed or by the Mann-Whitney U test when data were not normally distributed. The degree of correlation was evaluated by the coefficient of correlation (r) calculated using Pearson's correlation coefficient. Comparisons between three groups or more were made by one-way ANOVA followed by the Tukey test when data were normally distributed or by the Dunn's test when data were not normally distributed. The probability level is represented as the value *P*; statistical significance was set at $P<0.05$.

Results

Electrically evoked and light-evoked pupillary responses in normal subjects

Typical pupillary responses from a normal subject are shown in Fig. 4. The waveform of the EEPR was similar to that of the light response, but the amplitude of the EEPR was smaller than that of the light response. The mean latency of the EEPR (at 150 μA; 10 ms duration; 20 Hz; 20 pulses) was 0.29±0.01 s and that of the light response (660 nm; maximum light power of 10±3 μW; stimulus duration of 0.1 s) was 0.33±0.01 s. This difference was significant ($P<0.01$, Student's *t* test).

The relationship between the current intensity and EEPR was examined with stimuli of 20 Hz, 10 ms duration, and 20 pulses while the current intensity was varied from 25 μA to 250 μA. A RPC greater than 3% was obtained at currents ≥150 μA and the mean RPC was 6.3±1.1%. A highly significant positive correlation was found between the current intensity and the RPC amplitude ($r=0.98$ and $P<0.01$; Pearson's correlation coefficient, Fig. 5a).

We then examined the relationship between the frequency of the pulses and the EEPR at 150 μA, 10 ms duration and 20 pulses while the frequency of pulses varied from 5 Hz to 50 Hz. Although the mean RPC amplitude of the EEPR was very small at frequencies lower than 10 Hz, the mean RPC reached a peak of 7.9±1.9% at 20 Hz. Increasing the frequency up to 50 Hz resulted in a decrease in the RPC to 3.9±1.5% at 50 Hz (Fig. 5b).

The subjective phosphenes were brighter at frequencies between 15 and 33 Hz compared with those elicited by frequencies lower than 15 Hz or higher than 33 Hz.

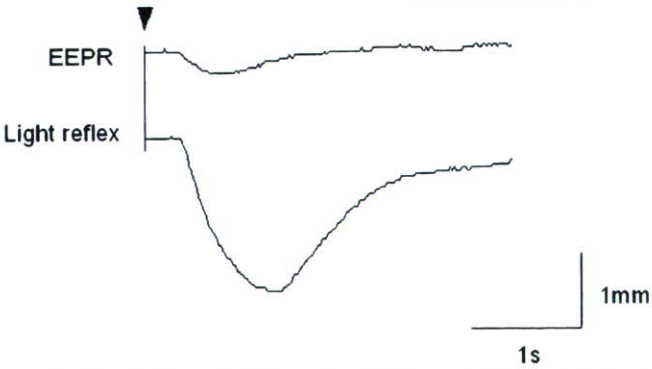

Fig. 4 Electrically evoked (upper) and light-evoked (lower) indirect pupillary responses elicited by electrical stimulation or light stimulation. The amplitude of the EEPR was smaller than that of light reflex, but the shape of the waveform is similar to that of light response

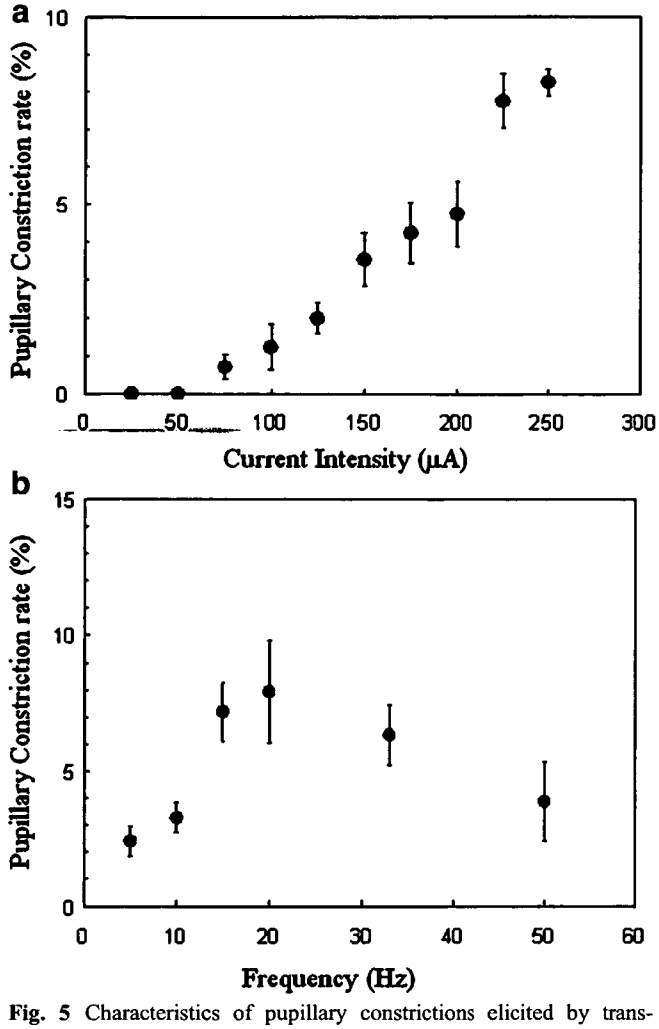

Fig. 5 Characteristics of pupillary constrictions elicited by transcorneal electrical stimulation. **a** Relative pupillary constriction amplitudes are plotted against the current intensity in normal subjects. The average pupillary constriction amplitude increases as the current intensity increases. **b** Relative pupillary constriction amplitudes are plotted against the frequency of electrical stimulation in normal subjects. A bandpass-shaped increase of pupillary constriction amplitude is observed. Bar represents standard error

Phosphenes evoked by trans-scleral electrical stimulation

All subjects reported a localized, round-shaped phosphene in response to TsES. The position of the phoshenes corresponded to the retinal loci where phoshenes were evoked by indenting the scleral electrode. Generally, shorter pulse durations elicited more localized phosphenes. The brightness of the phosphenes decreased with an increase of pulse duration in which the injected charge per pulse was kept constant (Fig. 6a). An increase in the interpulse delay also increased the perceived brightness of the phosphenes and was almost saturated at 1 ms (Fig. 6b). The brightness of the phosphenes increased with an increase in the pulse frequency up to 20 Hz and peaked at 50 Hz, but decreased at 100 Hz (Fig. 7a). With an increase in the pulse number, the brightness increased up to 20 pulses and saturated (Fig. 7b).

Phosphenes evoked by suprachoroidal-transretinal stimulation in patients with retinitis pigmentosa

Patient 1 (male) has had night blindness since age 7 years and progressive visual loss from 35 years. His visual acuity decreased to hand motion (OU) at the age of 50 years and was bare light perception (OU) at the time of phosphene test. TcES elicited phosphenes in the central visual field with a threshold current of 1.4 mA in the right eye. Patient 2 (female) has had night blindness from age 15 years and progressive visual loss from 27 years. Her visual acuity decreased to hand motion (OU) at the age of 55 years and was bare light perception (OD), and was 0 (OS) at the time of phosphene test. TcES elicited phosphenes that were perceived in the central visual field with a threshold current of 1.1 mA in the right eye.

Examination of the ocular fundus of the two patients with RP revealed extensive retinal degeneration including

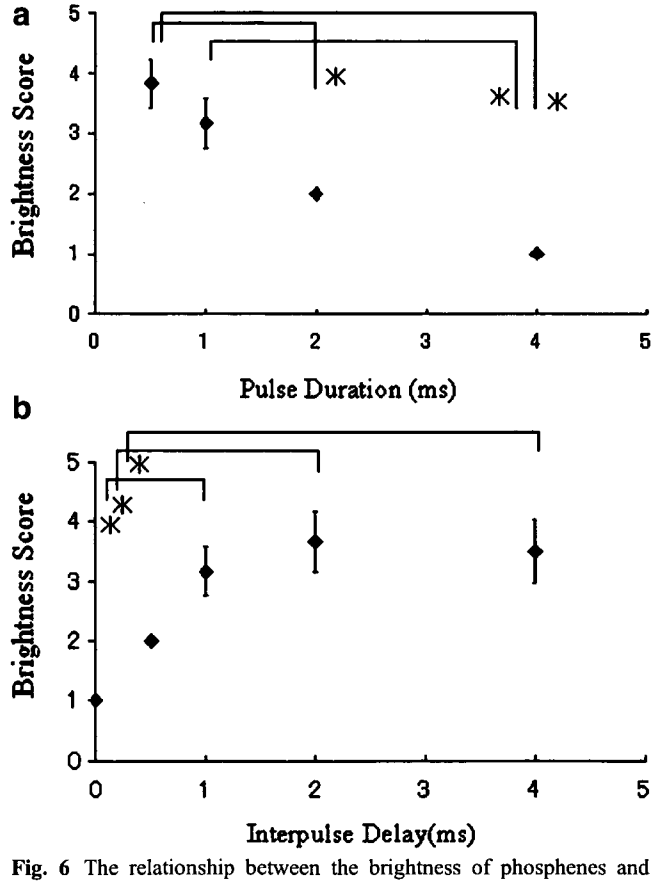

Fig. 6 The relationship between the brightness of phosphenes and pulse duration (**a**) and interpulse delay (**b**). **a** The brightness of phosphenes decreases with an increase of pulse duration (the total injected charge was constant). **b** The application of interpulse delay increased the perceived brightness of phosphene and almost saturated at 1 ms

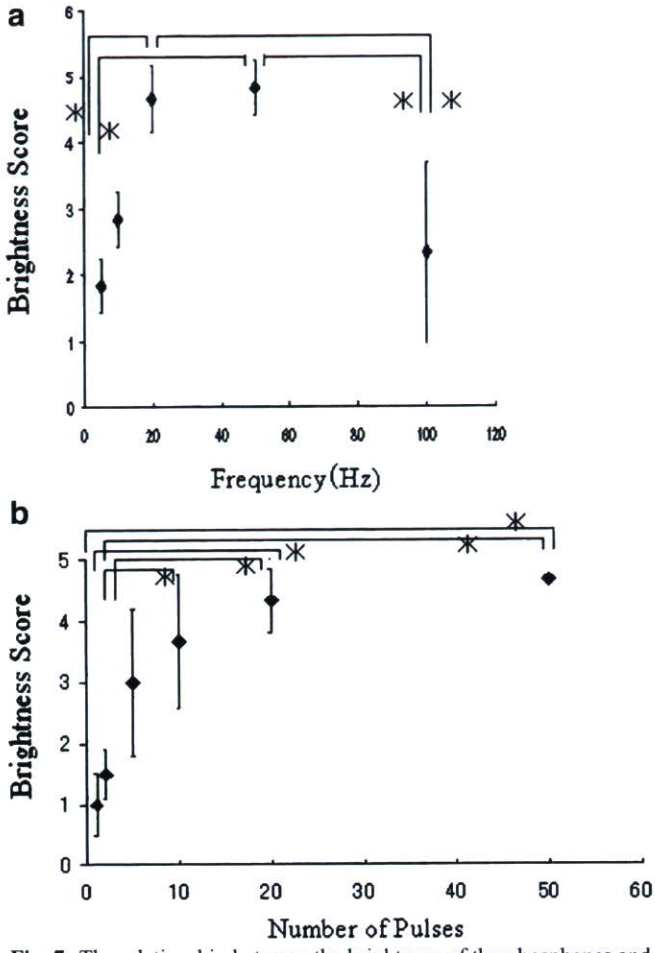

Fig. 7 The relationship between the brightness of the phosphenes and the pulse frequency (**a**) and the number of pulses (**b**). **a** The brightness of the phophenes increased with the increase of pulse frequency up to 20 Hz and peaked at 50 Hz, but decreased at 100 Hz. **b** With the increase of pulse number, the brightness increased up to 20 pulses and saturated. Bar represents standard error. $*P<0.05$

the macular and peripheral retina (Fig. 8). Trans-scleral monopolar stimulation revealed a confined low threshold area (0.4 mA, duration 1 ms) about 2 mm posterior to the inferior muscle insertion in patient 1. In patient 2, phosphenes were evoked from only a confined area about 2 mm posterior to the inferior muscle insertion with the maximum electrical current (1 mA, duration 1 ms).

By stimulating a single channel of nine electrodes with STS, localized phosphenes were obtained with stimuli of 0.3–0.5 mA (duration,0.5 ms: 0.48–0.80 mC/cm2) in patient 1 and 0.4 mA (duration,1.0 ms: 1.27 mC/cm2) in patient 2. Phosphenes were not reported from false-positive trials. Due to the difficulty in obtaining the results, only qualitative data can be provided in psychophysical experiments. The size of phosphene varied from a dime to a quarter coin at a distance of a stretched arm depending on the channel stimulated in both patients. Dumbbell-shaped phosphenes were perceived when the stimuli were delivered through two adjacent channels in both patients. Two dumbbell-shaped phosphenes oriented in different directions were perceived by stimulating different pairs of channels in patient 1.

Discussion

We have determined the efficient parameters to stimulate the retina by extraocular electrical stimuli. For TcES, two concentric ring electrodes were placed on the corneal surface and a current between the two rings has been reported to stimulate the peripheral retina by lower electrical currents and the macular area by higher currents [11]. The EEPR was used to evaluate the frequency dependence of TcES.

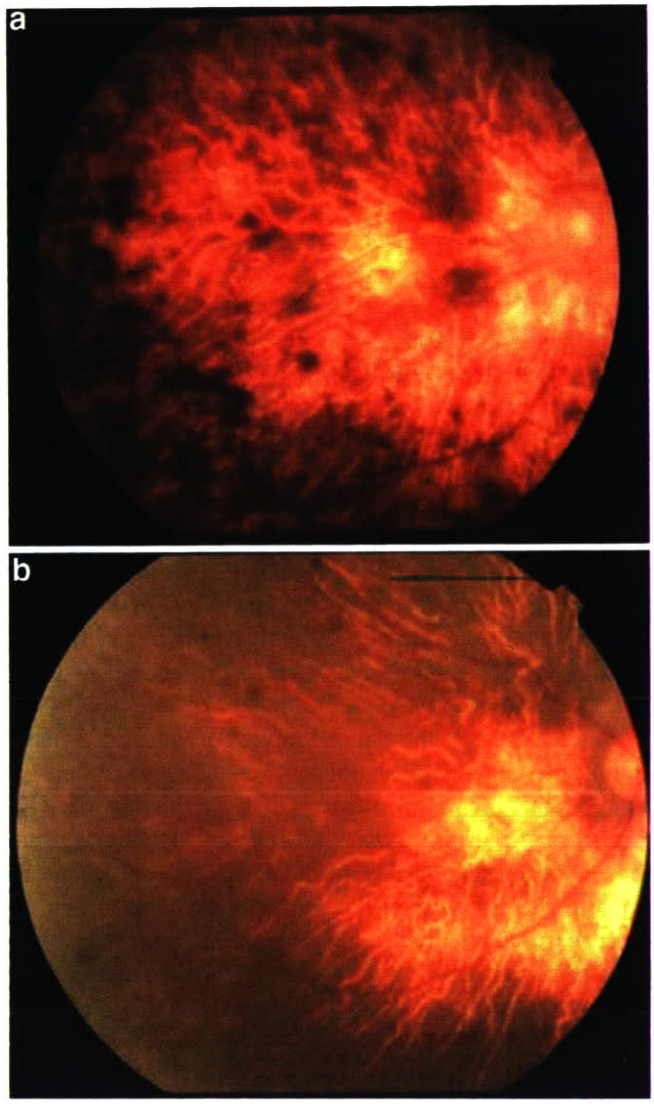

Fig. 8 Fundus photos of patient 1 (**a**) and patient 2 (**b**). In both patients, retinal degeneration can be seen in the macular area as well as in the peripheral retina

The relative amplitude of constriction of the EEPR increased as the current intensity increased, and the amplitude was largest at 20 Hz (Fig. 5). The perceived phosphene also became brighter around this frequency. These results together with previous reports [18, 28] suggest that a frequency around 20 Hz is the most effective frequency to stimulate the retina. The frequency dependency of the intensity of the phosphenes has not been explicitly reported, but for epiretinal stimulation, 20 Hz was used [22].

A possibility that a direct current affected the pupil efferent and elicited the EEPR was eliminated by the report that an EEPR cannot be elicited from the contralateral healthy eye from electrically stimulating an eye with optic atrophy [28].

The efficient parameters for localized extraocular stimulation for TsES were determined in normal subjects. The frequency dependence of the phosphene intensity showed a bandpass-shaped curve (Fig. 7), which was similar to the result of TcES. The peak EEPR was elicited by 20 Hz for TcES, while that for a subjective phophene was 50 Hz for TsES. This discrepancy may be because the EEPR was produced by the stimulation of W type RGCs [26], while the subjective phosphene was caused by X (alpha) or Y (beta) type RGCs [12, 26].

Shorter pulse durations elicited brighter phosphenes when the injected charge density was constant. These results are similar to those reported for epiretinal stimulation in electrophysiological experiment on rabbits [9] and on humans [22]. For the interpulse delay, the phosphene was brighter with a 1-ms delay compared with 0 or 0.5 ms. In epiretinal stimulation studies, 10 us to 2 ms were used [6, 22]. Pulse trains evoked brighter phosphenes than single-pulse stimulation. A pulse train (duration, 1.5 s) was also used in the epiretinal stimulation study [22]. From these findings, the efficient pulse parameters for extraocular stimulation in acute experiments may be a pulse duration of 0.5 to 1 ms, interpulse delay of 1 ms, frequency of 20 to 50 Hz and pulse number of 10 to 20.

In the acute experiment using STS on RP patients, the efficient parameters were used to maximize the efficacy of stimulation during the limited hours of an experiment. Transscleral monopolar stimulation was effective in finding the best area to create a scleral pocket for the implantation of the nine-channel electrode. The low threshold area corresponded anatomically to the macular area (just posterior to the insertion of inferior oblique muscle), which was consistent with the results of epiretinal prosthesis [7].

Localized phosphenes were elicited by the nine-channel STS system in two patients with advanced RP. Two-point discrimination (dumbbell-shaped phosphene) was also attained in the two patients, and primitive pattern recognition was obtained in patient 1. These results suggest that STS has the potential for being the basis for a pattern recognition system and be a feasible artificial vision system.

The charge densities to evoke phosphene by STS in two RP patients were 0.48 to 1.27 mC/cm2, which were comparable to the reported data of epiretinal stimulation, 0.28 to 2.88 mC/cm2 in RP patients using 400-um electrode [22].

In summary, biphasic pulses with a duration of 0.5–1.0 ms, interpulse delay of 1 ms, frequency of 20–50 Hz and trains of 10 to 20 were optimal for evoking phosphenes from localized extraocular stimulation. The STS using these parameters for advanced RP elicited localized phosphenes and enabled two-point discrimination, suggesting that STS is feasible as an approach to retinal prosthesis.

Acknowledgements The authors thank Yozo Miyake, Satoshi Suzuki, Mineo Kondo Yutaka Fukuda, Hajime Sawai and Tomomitsu Miyoshi for advice and discussion.

Commercial interest Hiroyuki Kanda and Motoki Ozawa are employees of the Nidek Company.

Financial support This study was supported by Health Sciences Research Grants (H16-sensory-001) from the Ministry of Health, Labor and Welfare, Japan.

References

1. Chow AY, Chow VY (1997) Subretinal electrical stimulation of the rabbit retina. Neurosci Lett 225:13–16
2. Chow AY, Chow VY, Packo KH, Pollack JS, Peyman GA, Schuchard R (2004) The artificial silicon retina microchip for the treatment of vision loss from retinitis pigmentosa. Arch Ophthalmol 122:460–469
3. Chowdhury V, Morley JW, Coroneo AM (2005) Stimulation of the retina with a multiekectrode extraocular visual prosthesis. ANZ J Surg 75:679–704
4. Hesse L, Schanze T, Wilms M, Eger M (2000) Implantation of retina stimulation electrodes and recording of electrical stimulation responses in the visual cortex of the cat. Graefe Arch Clin Exp Ophthalmol 238:840–845
5. Humayun MS, Price M, de Juan E Jr et al (1999) Morphometric analysis of the extramacular retina from postmortem eyes with retinitis pigmentosa. Invest Ophthalmol Vis Sci 40:143–148
6. Humayun MS, de Juan E, Weiland JD, Dagnelie G, Katona S, Greenberg R, Suzuki S (1999) Pattern electrical stimulation of human retina. Vision Res 39:2569–2576
7. Humayun MS, Weiland JD, Fujii GY, Greenberg R, Williamson R, Little J, Mech B, Cimmarusti V, Van Boemel G, Dagnelie G, de Juan E (2003) Visual perception in a blind subject with a chronic microelectronic retinal prosthesis. Vision Res 43:2573–2581
8. Jensen RJ, Rizzo JF 3rd, Ziv OR, Grumet A, Wyatt J (2003) Thresholds for activation of rabbit retinal ganglion cells with an ultrafine, extracellular microelectrode. Invest Ophthalmol Vis Sci 44:3533–3543
9. Jensen RJ, Ziv OR, Rizzo JF 3rd (2005) Thresholds for activation of rabbit retinal ganglion cells with relatively large, extreacellular microelectrodes. Invest Ophthalmol Vis Sci 46:1486–1496
10. Kanda H, Morimoto T, Fujikado T, Tano Y, Fukuda Y, Sawai H (2004) Electrophysiological studies on the feasibility of suprachoroidal-transretinal stimulation for artificial vision in normal and RCS Rat. Invest Ophthalmol Vis Sci 45:560–566

11. Kawasumi M (1981) Distribution of current intensities inside the electrically stimulated eye. Nippon Ganka Gakkai Zasshi 89:766–772
12. Leventhal AG, Rodieck RW, Dreher B (1981) Retinal ganglion cell classes in the old world monkey: morphology and central projections. Science 213:1139–1142
13. Majji AB, Humayun MS, Weiland JD, Suzuki S, D'Anna SA, de Juan E Jr (1999) Long-term histological and electrophysiological results of an inactive epiretinal electrode array implantation in dogs. Invest Ophthalmol Vis Sci 40:2073–2081
14. Margalit E, Maia M, Weiland JD, Greenberg RJ, Fujii GY, Torres G, Piyathaisere DV, O'Hearn TM, Liu W, Lazzi G, Dagnelie G, Scribner DA, de Juan E Jr, Humayun MS (2002) Retinal prosthesis for the blind. Surv Ophthalmol 47:335–356
15. Marmor MF, Aguirre G, Arden G et al (1983) Retinitis pigmentosa: a symposium on terminology and methods of examination. Ophthalmology 90:126–131
16. Miyake Y, Yanagida K, Yagasaki K (1980) Clinical application of EER (electrically evoked response) (2) Analysis of EER in patients with dysfunctional rod or cone visual pathway. Nippon Ganka Gakkai Zasshi 84:502–509
17. Morimoto T, Fukui T, Matsushita K, Okawa Y, Shimojyo H, Kusaka S, Tano Y, Fujikado T (2006) Evaluation of residual retinal function by pupillary constrictions and phosphenes using transcorneal electrical stimulation in patients with retinal degeneration. Graefe Arch Clin Exp Ophthalmol 244:1283–1292
18. Motokawa K, Ebe M (1952) Selective stimulation of color receptors with alternating currents. Science 25(115):92–94
19. Nakauchi K, Fujikado T, Kanda H, Morimoto T, Choi JS, Ikuno Y, Sakaguchi H, Kamei M, Ohji M, Yagi T, Nishimura S, Sawai H, Fukuda Y, Tano Y (2005) Transretinal electrical stimulation by an intrascleral multichannel electrode array in rabbit eyes. Graefe Arch Clin Exp Ophthalmol 243:169–174
20. Pagon RA (1988) Retinitis pigmentosa. Surv Ophthalmol 33:137–177
21. Potts AM, Inoue J (1969) The electrically evoked response of the visual system (EER) II. Effect of adaptation and retinitis pigmentosa. Invest Ophthalmol 8:605–613
22. Rizzo JF 3rd, Wyatt J, Loewenstein J, Kelly S, Shire D (2003) Method and perceptual threshold for short-term electrical stimulation of human retina with a microelectrode array. Invest Ophthalmol Vis Sci 44:5355–5361
23. Rizzo JF 3rd, Wyatt J, Loewenstein J, Kelly S, Shire D (2003) Perceptual efficacy of electrical stimulation of human retina with a microelectrode array during short-term surgical trials. Invest Ophthalmol Vis Sci 44:5362–5369
24. Santos A, Humayun MS, de Juan E Jr, Greenburg RJ, Marsh MJ, Klock IB, Milam AH (1997) Preservation of the inner retina in retinitis pigmentosa: a morphometric analysis. Arch Ophthalmol 115:511–515
25. Schwahn HN, Gekeler F, Kohler K, Kobuch K, Sachs HG, Schulmeyer F, Jakob W, Gabel VP, Zrenner E, Schwahn HN (2001) Studies on the feasibility of a subretinal visual prosthesis: data from Yucatan micropig and rabbit. Graefe Arch Clin Exp Ophthalmol 239:961–967
26. Stone J, Fukuda Y (1974) Properties of cat's retinal ganglion cells: a comparison of W-cells with X-cells and Y-cells. J Neurophysiol 37:722–748
27. Stone JL, Barlow WE, Humayun MS, de Juan E Jr, Milam AH (1992) Morphometric analysis of macular photoreceptors and ganglion cells in retinas with retinitis pigmentosa. Arch Ophthalmol 110:1634–1639
28. Tanino T, Kato S, Kawasumi M (1981) Studies on electrically evoked pupillary reflex-Indirect reflex and its frequency characteristics. Jpn J Ophthalmol 25:423–429
29. Veraart C, Raftopoulos C, Mortimer JT, Delbeke J, Pins D, Michaux G, Vanlierde A, Parrini S, Wanet-Defalque MC (1998) Visual sensations produced by optic nerve stimulation using an implanted self-sizing spiral cuff electrode. Brain Res 813:181–186
30. Walter P, Heimann K (2000) Evoked cortical potentials after electrical stimulation of the inner retina in rabbits. Graefe Arch Clin Exp Ophthalmol 238:315–318
31. Zrenner E (2002) Will retinal implants restore vision? Science 295:1022–1025

Optical Imaging to Evaluate Retinal Activation by Electrical Currents Using Suprachoroidal-Transretinal Stimulation

Yoshitaka Okawa,[1] Takashi Fujikado,[1] Tomomitsu Miyoshi,[2] Hajime Sawai,[2] Shunji Kusaka,[1] Toshifumi Mihashi,[3] Yoko Hirohara,[3] and Yasuo Tano[4]

Purpose. To determine whether reflectance changes of the retina after electrical suprachoroidal-transretinal stimulation (STS) can be detected with a newly developed optical imaging fundus camera.

Methods. Ten eyes of 10 cats were studied. A small retinal area was focally stimulated with electric currents passing between an active electrode placed in the fenestrated sclera and a reference electrode in the vitreous. Biphasic pulses were applied for 4 seconds with a current up to 500 μA. Images of the fundus illuminated with near-infrared (800–880 nm) light were obtained every 20 msec for 26 seconds between 2 seconds before and 20 seconds after the STS. Twenty images of 20 consecutive experiments were averaged. A two-dimensional map of the reflectance changes was constructed by subtracting the images before the stimulation from those after the stimulation. STS-evoked potentials (EPs) were recorded from the optic chiasma.

Results. Approximately 0.5 second after the onset of STS, reflectance changes were observed around the retinal locus, where the stimulating electrodes were positioned. The intensity of the reflectance changes was correlated with the intensity of the stimulus current. The area of the reflectance change increased as the current intensity increased and was correlated with the amplitude of the EPs ($R^2 = 0.82$).

Conclusions. Reflectance changes after STS were localized to the area around the electrode. The strong correlation between the area of the reflectance changes and the amplitude of the EPs suggested that the reflectance changes reflected the activity of retinal neurons elicited by electrical stimulation. (*Invest Ophthalmol Vis Sci.* 2007;48: 4777–4784) DOI:10.1167/iovs.07-0209

From the Departments of [1]Applied Visual Science, [2]Physiology, and [4]Ophthalmology, Osaka University Graduate School of Medicine, Suita, Japan; and [3]Topcon Research Institute, Itabashi, Japan.

Supported by Health Sciences Research Grants (H16-sensory-001) from the Ministry of Health, Labor and Welfare, Japan and by Grant 18591918 from the Ministry of Education, Culture, Science and Technology.

Submitted for publication February 18, 2007; revised May 21, 2007; accepted August 10, 2007.

Disclosure: **Y. Okawa**, None; **T. Fujikado**, None; **T. Miyoshi**, None; **H. Sawai**, None; **S. Kusaka**, None; **T. Mihashi**, Topcon Research Institute (E); **Y. Hirohara**, Topcon Research Institute (E); **Y. Tano**, None

The publication costs of this article were defrayed in part by page charge payment. This article must therefore be marked "*advertisement*" in accordance with 18 U.S.C. §1734 solely to indicate this fact.

Corresponding author: Takashi Fujikado, Department of Applied Visual Science, Osaka University Graduate School of Medicine, 2-2 Yamadaoka, Suita, Osaka 565-0871, Japan; fujikado@ophthal.med.osaka-u.ac.jp.

In vivo optical imaging of intrinsic signals is a well-established method to study brain physiology and to map the functional architecture of the cerebral cortex.[1–4] In optical imaging studies, stimulus-induced neuronal activity is detected as a change of light reflectance. The reflectance change does not directly indicate neural activation, but it is strongly correlated with the activity of neurons examined by conventional extracellular recordings.[5] Studies of cortical optical imaging have shown that this intrinsic signal originates from stimulus-induced changes in the light-scattering of neural tissues and from changes in light absorption associated with hemodynamic changes in blood volume or the oxygenated state of hemoglobin.[6,7]

Recently, the technique of optical imaging has been applied to the retina to examine light-evoked reflectance changes.[8–10] Although the light-evoked neuronal activity in localized areas of the retina can be recorded by multifocal electroretinography (mfERG),[11] those evoked by electrical stimulation are difficult to detect by mfERG because of the large stimulus artifact. Therefore, optical recording is a reasonable alternative to study the responses evoked by the electrical stimulation of the retina.

Artificial retinas, also called retinal prostheses, have been placed at different sites.[12–15] A typical retinal prosthesis consists of an array of electrodes implanted above (epi-) or beneath (sub-) the retina and is used to deliver electrical current to the retina to evoke a light sensation called a phosphene. We have implanted an electrode array in the suprachoroidal space, and stimulation by this system has been called suprachoroidal-transretinal stimulation (STS).[16] In STS, the active electrode array is placed in the fenestrated sclera in the retrobulbar space while the reference electrode is inserted into the vitreous cavity. STS is a safe method and avoids the direct contact of electrodes with the retina, but the distance between electrodes and retina is larger than in the epiretinal or subretinal methods. Thus, it is necessary to determine whether sufficient spatial resolution can be achieved by this approach.

The spatial resolution of epiretinal electrodes has been investigated by optical imaging in the visual cortex[17] but not in the retina. The purpose of this study was to determine whether reflectance changes can be detected in the area of the retina activated by STS. To accomplish this, we have developed a prototype optical-imaging fundus camera to measure the changes of light reflectance evoked by electrical stimulation of the retina.

Materials and Methods

Animals

Ten left eyes of 10 cats under general anesthesia were used. Cat 1 was used for the study of light stimulation, and cats 2 through 10 were used for the electrical stimulation. Cats 6, 7, and 9 were also used for the study of evoked potential (EP) at optic chiasm. Initially, each animal received an intramuscular injection of ketamine hydrochloride (25

mg/kg) and an intraperitoneal injection of atropine sulfate (0.1 mg/kg). Then each animal was anesthetized by intravenous infusion of pentobarbital sodium (1 mg/kg per hour) and paralyzed by pancuronium bromide (0.2 mg/kg per hour) mixed with Ringer solution and glucose (0.1 g/kg per hour).

The animal was artificially ventilated with a mixture of N_2O/O_2 (1:1), and the end-tidal CO_2 concentration was controlled at 3.5% to 5.0% by altering the frequency and volume of ventilation. In addition to the continuous monitoring of the expired CO_2, the intratracheal pressure and electrocardiogram were also monitored. Body temperature was maintained with a heating pad at 38°C.

Surgical Procedures

An incision was made over the temporal area of the left eye; part of the lateral orbital wall (zygomatic and frontal bone) was removed, and the lateral rectus muscle was dissected. The scleral area just above the long ciliary artery was exposed, and a 3- to 4-mm incision was made through the sclera. The conjunctiva was sutured to a fixed frame attached to the stereotaxic headholder to prevent eye movements. The pupil was dilated with 5% phenylephrine hydrochloride, 0.5% tropicamide, and 1% atropine sulfate. To protect the corneal surface, a hard contact lens was placed on the cornea (polymethylmethacrylate; base curve, 8.50 mm; power, +1.5 D; diameter, 13.5 mm). All experiments were performed in accordance with the ARVO Statement for the Use of Animals in Ophthalmic and Visual Research, and the procedures were approved by the Animal Research Committee of Osaka University Medical School.

Optical Imaging of Retina

The ocular fundus was monitored by a fundus camera (TRC-50LX; Topcon Corp., Tokyo, Japan) with a digital CCD camera (C8484; Hamamatsu Photonics, Hamamatsu, Japan). The number of pixels was 1280 × 1024, but the binning mode of the camera was used to obtain maximum light sensitivity and the resolution was reduced to 320 × 256 pixels (12-bit grayscale). A 12-bit digitizer was used, and the 4096 grayscale levels were obtained for each pixel.

A halogen lamp was used to illuminate the posterior fundus, and a bandpass filter was inserted in the illumination optical path to limit the wavelength of the fundus monitoring light between 800 and 880 nm. The power of the illuminating light was 250 nW, which was much lower than the safe exposure limit decided by American National Standard Institute.

To improve the signal-to-noise ratio, 20 images of 20 consecutive experiments were averaged (Fig. 1). The interval between each session was 1 minute. A two-dimensional image of the optical signal was obtained by subtracting the image recorded before stimulation from those after stimulation. All experiments were performed in a dark room after 30 minutes of dark adaptation.

Electrophysiological Recording from Optic Chiasma

To record the potentials evoked by electrical stimulation of the retina from the optic chiasma (OX), a pair of stainless steel electrodes was placed in the OX stereotaxically. Light-evoked responses were recorded from each electrode to be certain that the electrodes were placed in the OX.

To record the electrically evoked potentials (EEPs), the signal was amplified 10,000 times and was bandpass filtered between 300 Hz and 5 kHz with an AC amplifier (model 1800; Microelectrode AC amplifier; A-M Systems, Inc., Carlsborg, WA) and a signal conditioner (LPF-202A; Warner Instruments, Hamden, CT). Amplified EEPs were fed to a signal processor (Power 1401; Cambridge Electronic Design, Cambridge, UK) with a sampling frequency of 50 kHz and were analyzed off-line. Signals were also monitored on an oscilloscope and an audio speaker in real time.

Focal Light Stimulation of Retina

The stimuli were obtained from white light-emitting diodes controlled by a pulse generator. The stimulating light was a vertical bar focused on the retina, flickering at 8 Hz for 4 seconds. The width of the bar was 4°, and the center of the bar was located 6° temporal to the fovea (Fig. 2A). The light power was 30 nW. Images were obtained every 20 msec for 18 seconds between 2 seconds before and 12 seconds after the stimulus.

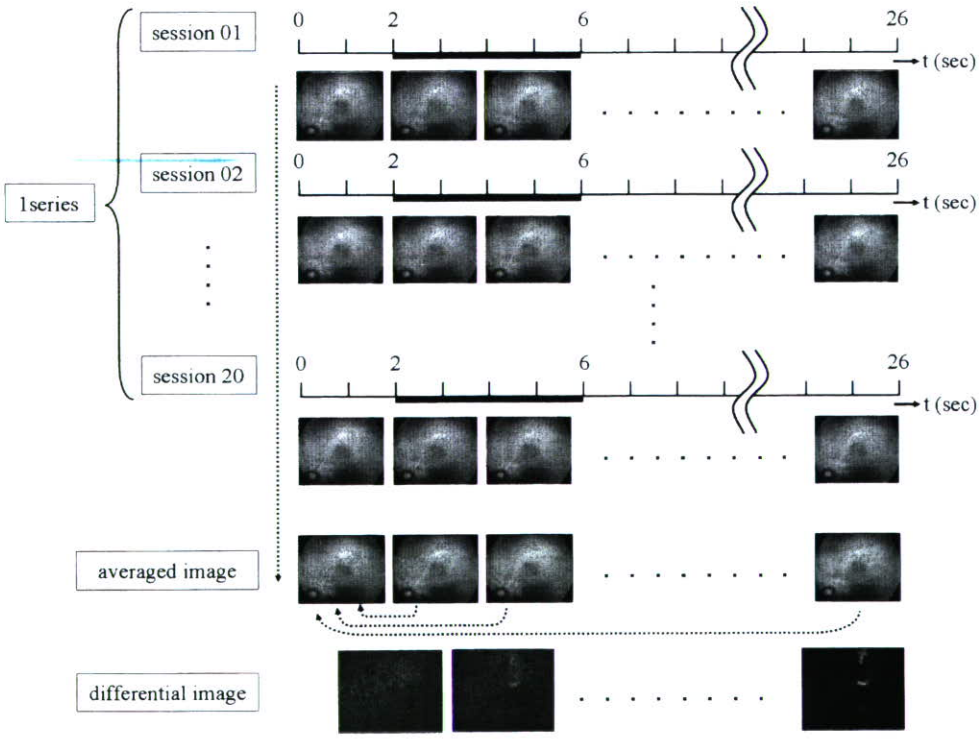

FIGURE 1. Sequence of image processing for optical imaging in this experiment.

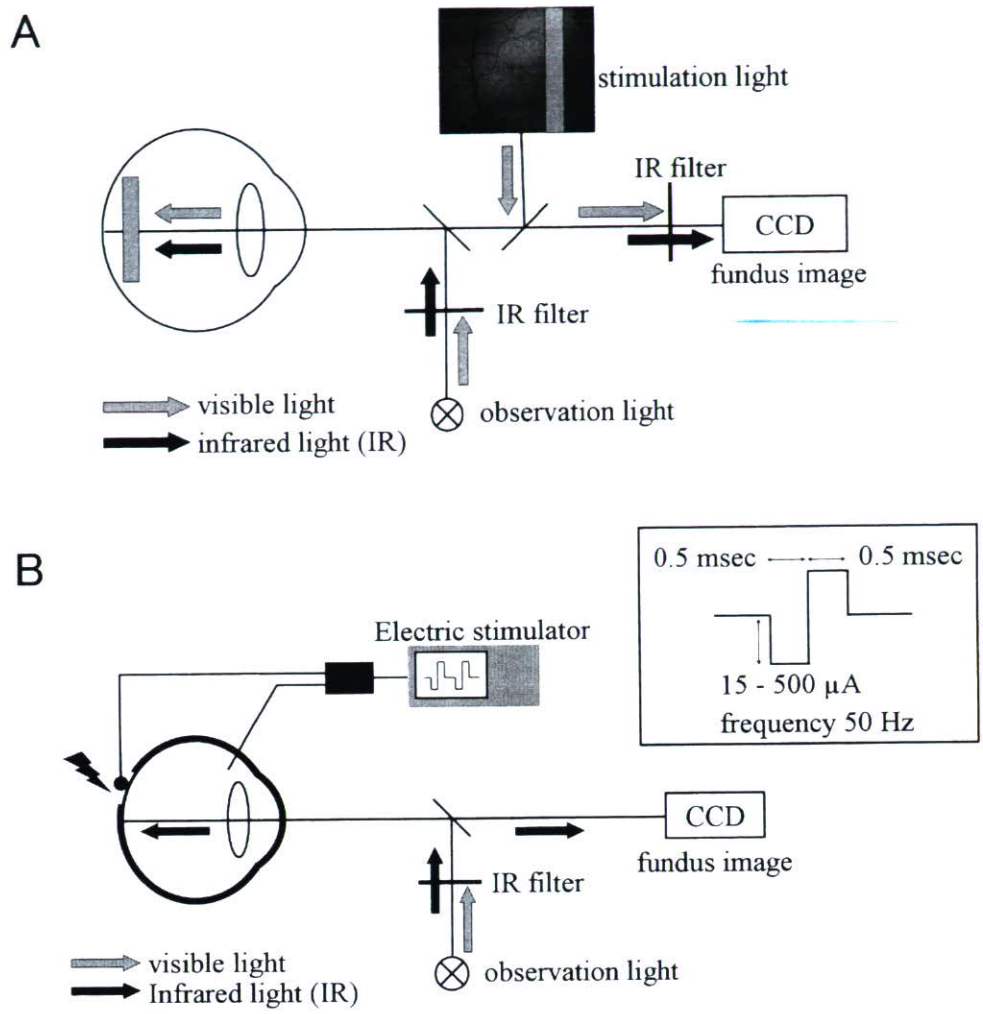

FIGURE 2. Schema of optical imaging for light stimulation (**A**) and for STS (**B**).

Focal Electrical Stimulation of Retina

A single-channel platinum electrode (diameter, 100 μm) was used as the active scleral electrode. A vitreous electrode was inserted into the vitreous through the sclera at the pars plana. This electrode was a urethane-coated platinum wire (0.2 mm in diameter), and its exposed tip measured approximately 2 mm. The active electrode was held gently against the sclera by a manipulator, and the pressure on the eye was minimal, as determined by the degree of indentation of the retina viewed by the fundus camera. The mass EP at the OX elicited by STS was also monitored to confirm the effectiveness of the electrical stimulation.

For each STS trial, biphasic pulse trains (outward first) were applied at 50-Hz frequency, 0.5-msec pulse duration, and 4-second stimulation (Fig. 2B). All pulses were generated by a pulse generator (SEN7203; Nihon Kohden Corp., Tokyo, Japan) and were delivered to the electrodes through a linear stimulus isolation unit (BSI-950; Dagan Corporation, Minneapolis, MN).

To evaluate the correlation between the stimulus current and the area of reflectance change, the stimulating current was increased systematically between the threshold current to the maximum current (≤500 mA) or decreased systematically to examine hysteresis. Images were obtained every 20 msec for 26 seconds between 2 seconds before and 20 seconds after the electrical stimulation.

Data Analyses

Optical Density Measurements. To evaluate the intensity of the reflectance, the grayscale value (GSV) of each spot in the focused area was averaged. The averaged GSV of each spot after the onset of light or electrical stimulation was subtracted from that before the electrical stimulation to obtain the differential image (Fig. 1). For the evaluation of the area of reflectance change, the GSV value of 40 (approximately 8 SD of the GSV without stimulation) was set as the cutoff level to reduce the effect of baseline fluctuations. To study the relationship between the area of reflectance change (pixels) and the stimulus current, the maximum number of pixels in which the averaged reflectance change exceeded the cutoff level (±40 GSV) during the time course was selected to determine the maximum area of reflectance change. The number of pixels with an increase or a decrease of reflectance was added to evaluate the area of retinal excitation.

Electrophysiological Measurements. The amplitude of the EPs evoked by STS was determined by measuring the amplitude between the first negative peak (latency approximately 3.0 msec) and the second positive peak (latency approximately 4.0 msec). Two hundred records were averaged to determine the amplitude for a particular stimulus current.

Statistical Analysis

Regression analysis between the stimulus current and the area of reflectance change or the amplitude of EP at OX was evaluated by SPSS (SPSS Inc., Chicago, IL).

RESULTS

Optical Imaging after Light Stimulation

Examination of a two-dimensional map of the reflectance changes after light stimulation showed that the reflectance

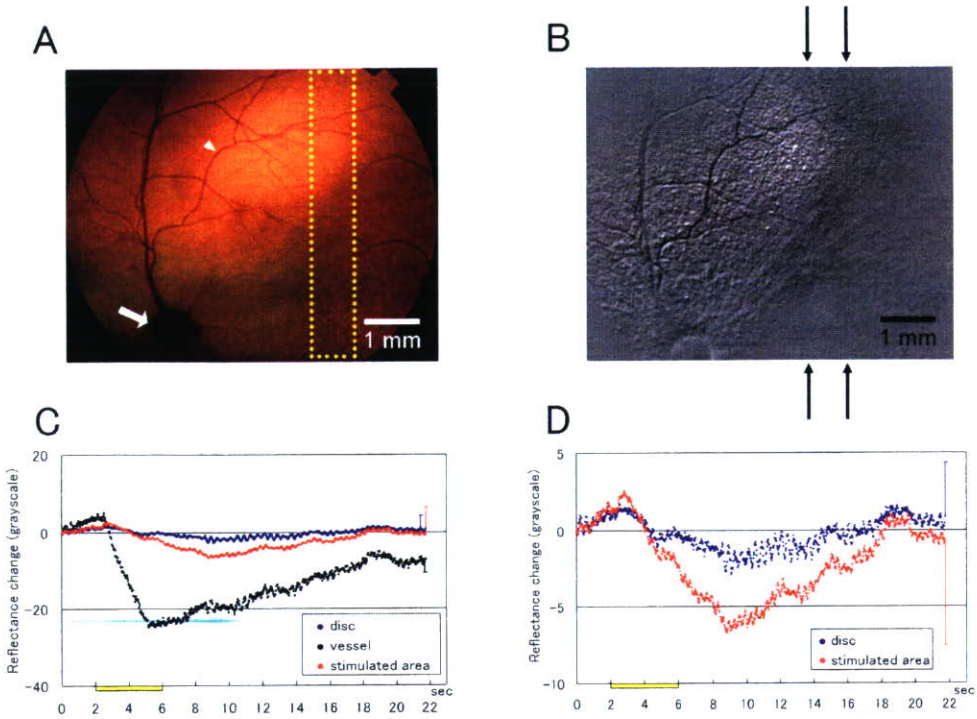

FIGURE 3. Results of optical imaging for light stimulation. (**A**) Color fundus photograph of cat retina. (**B**) Two-dimensional map of reflectance changes (differential map) 3 seconds after the onset of light stimulation. *Black arrows*: area of light stimulation. (**C**) Changes of light reflectance at the blood vessel (*black line*), at optic disc (*blue line*), and at stimulated retinal area (*red line*). (**D**) Magnified image of (**C**). (**A**) Area of reflectance change measured for the blood vessel (*arrowhead*), optic disc (*arrow*), and retina (*yellow dots*). (**C**, **D**) *Yellow bar*: period of light stimulation. (**A**, **B**) *Bars*: scale of ocular fundus. (**C**, **D**) *Bars*: SD of reflectance change.

decreased in the stimulated striped area (Fig. 3). Reflectance of the retinal vessels began to decrease approximately 0.5 second after the stimulus onset and continued to decrease linearly to a deep trough at approximately 3.5 seconds (Fig. 3C). The change of reflectance of the optic disc and stimulated retinal area showed similar temporal changes. Reflectance began to decrease approximately 1.0 second after the stimulus onset and continued to decrease almost linearly to a deep trough at approximately 7.0 seconds after the stimulus onset (Fig. 3D).

Optical Imaging of STS

A two-dimensional map of the reflectance changes after electrical stimulation showed an increase of reflectance in the retinal area, where the tip of the electrode was attached to the sclera. A decrease of reflectance was observed in the retinal area surrounding the area of increased reflectance (Fig. 4; see also Fig. 7A). The time course of the reflectance changes was similar with the different intensities of electrical stimulation.

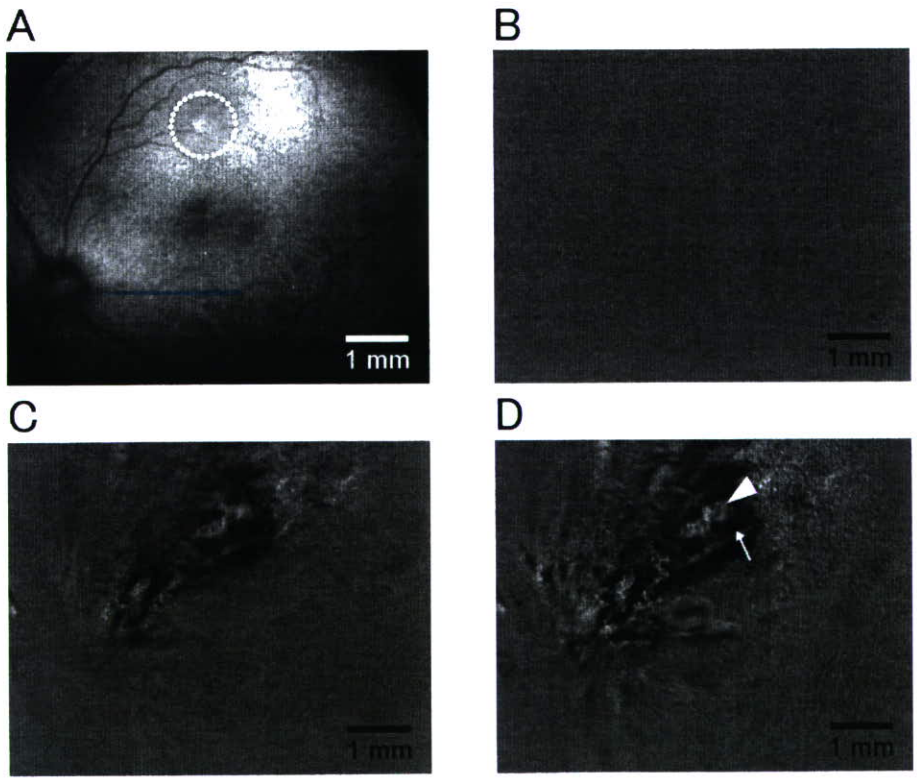

FIGURE 4. Results of optical imaging for electrical stimulation. (**A**) Fundus photograph of a cat retina with an electrode attached to the hemidissected sclera. *Dotted white circle*: position of the electrode. (**B**–**D**) Differential map of the reflectance change 2 seconds after the onset of electrical stimulation. (**B**) No stimulation. (**C**) Stimulus current of 125 μA. (**D**) Stimulus current of 250 μA. *Arrowhead*: high-reflectance area at the electrode. *Arrow*: low-reflectance area surrounding the electrode. (**A**–**D**) *Bars*: scale of ocular fundus.

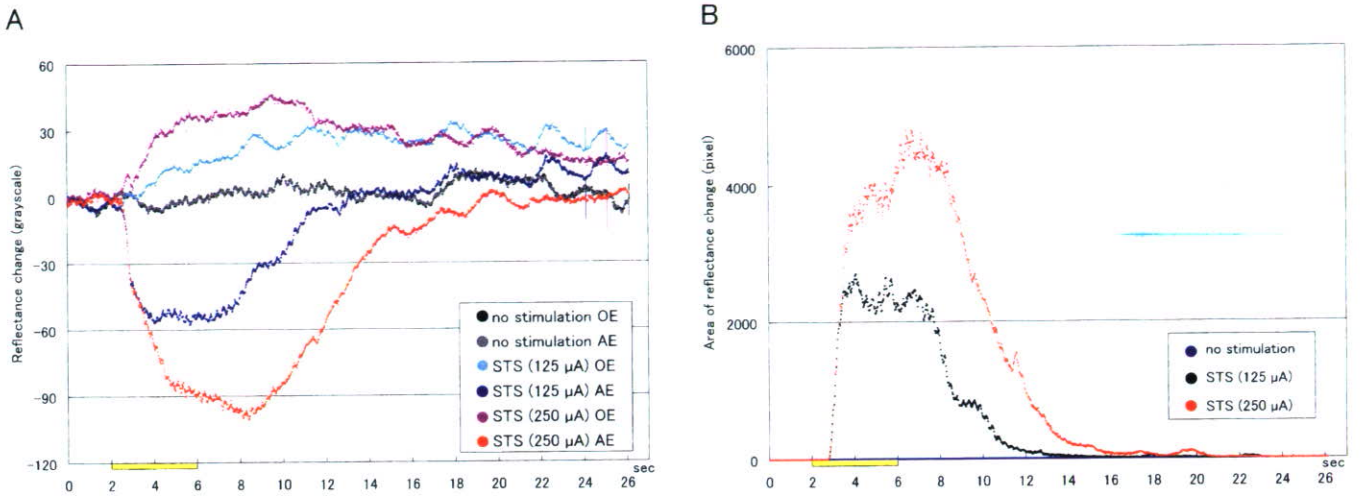

FIGURE 5. Time course of the intensity of reflectance change (**A**) and the area of reflectance change (**B**) in cat 2. (**A**) Intensity (gray scale) of reflectance change with currents of (*red line*) 250 μA and (*dark blue line*) 125 μA around the electrode (AE). Reflectance change with currents of (*purple line*) 250 μA and (*light blue line*) 125 μA on the electrode (OE). *Black line*: reflectance change OE without electrical stimulation. *Bar*: SD of reflectance change. (**B**) Area (pixels) of reflectance change with currents of (*red line*) 250 μA and (*black line*) 125 μA and with (*blue line*) no stimulation.

The increase at the electrode or the decrease surrounding the electrode of light reflectance was observed approximately 0.5 second after the stimulus onset, increased or decreased rapidly for 1.5 to 2.0 seconds, increased or decreased gradually to peak at 4 to 6 seconds after stimulus onset, and then returned to the baseline gradually (Figs. 5A, 6A). Reflectance did not change at the electrode site when stimulation was not applied (Fig. 5A). The maximum value of reflectance increase on the electrode or reflectance decrease around the electrode was linearly related to the increase of stimulus intensity (Fig. 6B).

The area of the reflectance change (increased and decreased reflectance areas were combined) had a similar time course with different stimulus intensities. The area began to increase approximately 0.5 second to 1.0 second after stimulus onset and changed linearly for 1.0 to 1.5 seconds The size of the area peaked 2 to 5 seconds after stimulus onset, was sustained for 4 to 8 seconds, and returned to the baseline gradually (Figs. 5B, 7B). The area of the reflectance changes increased with an increase of current intensity (Fig. 7C). Reflectance changes on and around the electrode were not observed when stimulation was not applied (Fig. 5B).

The threshold current for eliciting a reflectance change ranged from 65 μA to 200 μA for the different cats. Linear regression analysis showed that R^2 ranged from 0.82 to 0.97 in the 9 cats (cats 2–10), suggesting that the area of reflectance changed linearly with the stimulus current intensity. The slope of the regression line varied in the different cats (Fig. 8).

Electrophysiological Recordings from Optic Chiasm after STS

We examined the relationship between the EP amplitude recorded in the OX and the stimulus current in three cats (cats 6, 7, 9; Fig. 9). EP amplitude increased linearly with an increase of stimulus current (Fig. 10). Linear regression analysis showed the R^2 values were 0.89, 0.95, and 0.98, respectively, suggest-

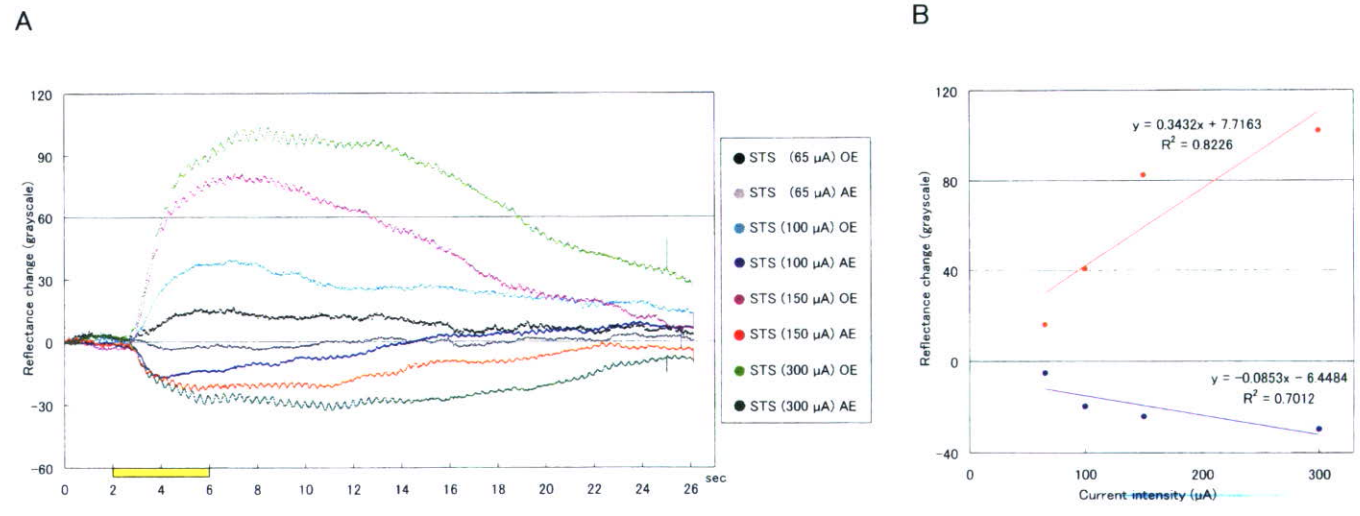

FIGURE 6. Time course of the reflectance change in cat 3. (**A**) Time course of the intensity of reflectance change. (**B**) Relationship between the maximum intensity of reflectance change and the stimulus current. (**A**) Reflectance change with currents of (*green line*) 300 μA, (*purple line*) 150 μA, (*light blue line*) 100 μA, and (*black line*) 65 μA on electrodes. Reflectance change with currents of (*dark green line*) 300 μA, (*red line*) 150 μA, (*dark blue line*) 100 μA, (*gray line*) and 65 μA around electrodes. (**B**) Linear regression line of maximum reflectance change (*red line*) on the electrode and (*blue line*) around the electrode. (**A**) *Bar*: SD of reflectance change.

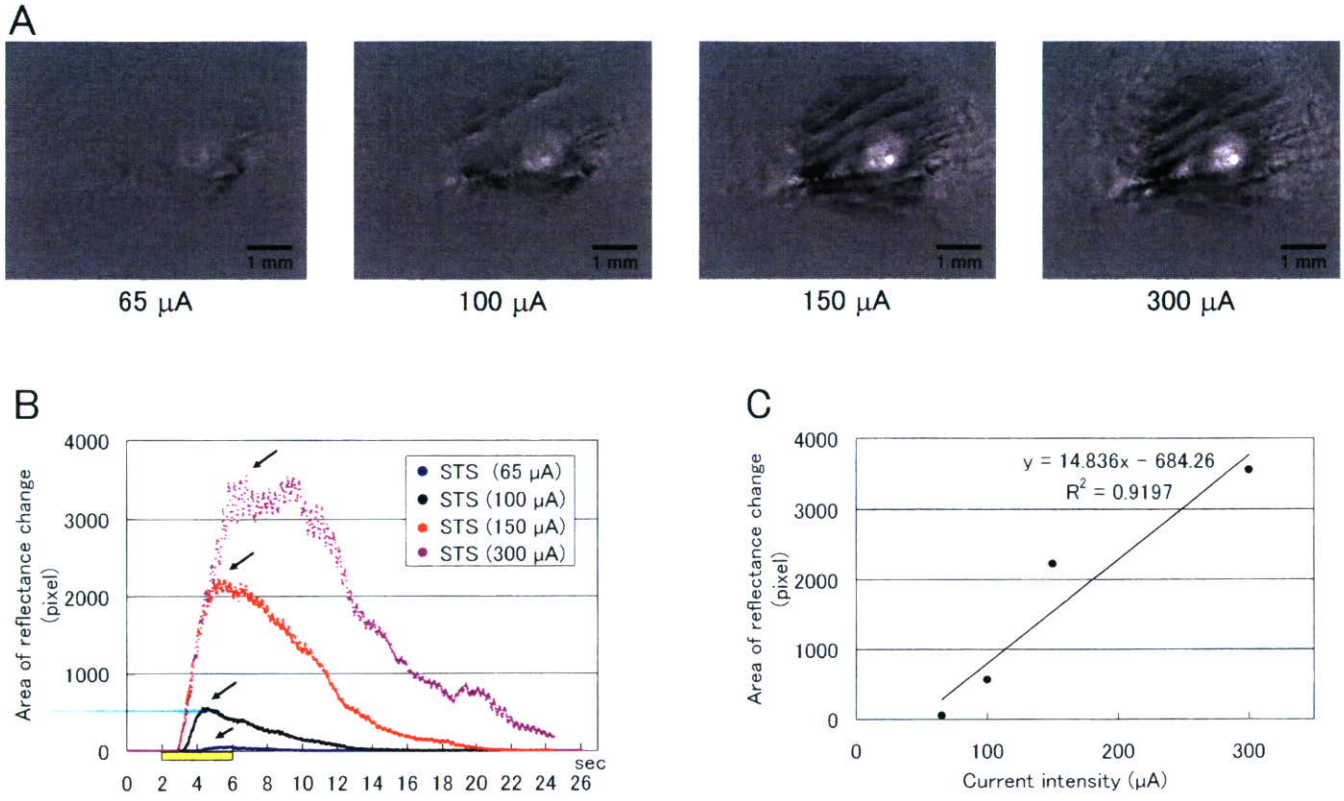

FIGURE 7. The area of reflectance change in relation to the electrical current in cat 3. (**A**) Differential image of the reflectance changes of the retina 2.4 seconds after the onset of electrical stimulation with an electrical current from 65 μA to 300 μA. (**B**) Time course of the area (pixels) of reflectance change with different stimulus currents. *Purple*, 300 μA; *red*, 150 μA; *black*, 100 μA; *blue*, 65 μA. (**C**) Relationship between the maximum area of reflectance change (pixels) and the stimulus current. (**A**) *Bars*: scale of ocular fundus.

ing that the EP changed linearly with the stimulus current intensity. The slope of the regression line varied in the different cats (data are not shown).

The relationship between the amplitude of EP and the area of reflectance change was also assessed in cats 6, 7, and 9. Linear regression analysis showed that the R^2 values were 0.82, 0.84, and 0.82, respectively, suggesting that the reflectance changed linearly with the EP at OX through electrical stimulation to the retina (Fig. 10).

DISCUSSION

We have developed an optical imaging system to evaluate the retinal area activated by focal electrical stimulation to the

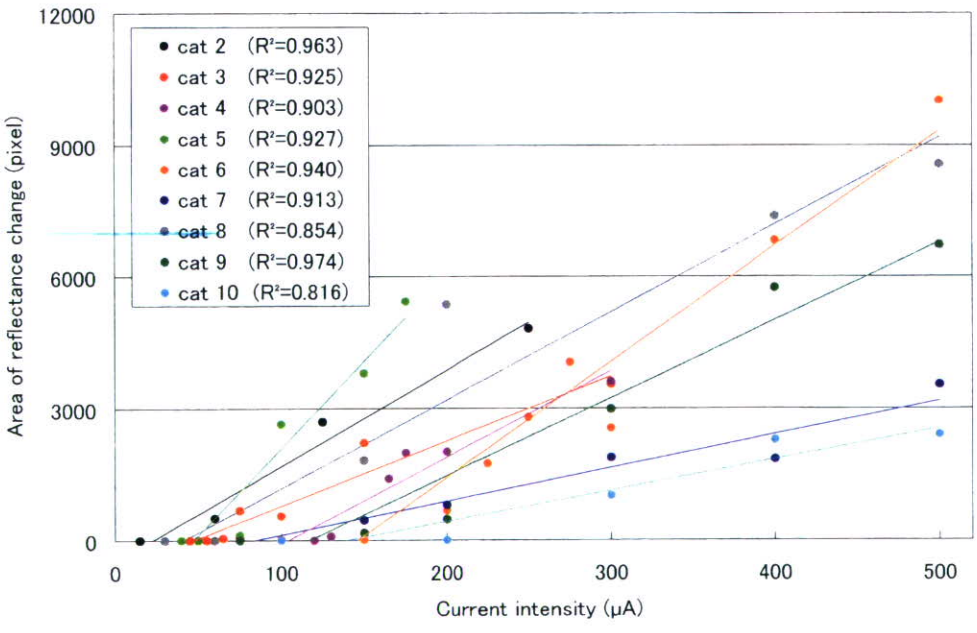

FIGURE 8. Relationship between the area of reflectance change (pixels) and the stimulus current in cats 2 to 10. Each point represents the maximum number of pixels during or after electrical stimulation in which the reflectance change exceeded the cutoff level (gray scale value of 40).

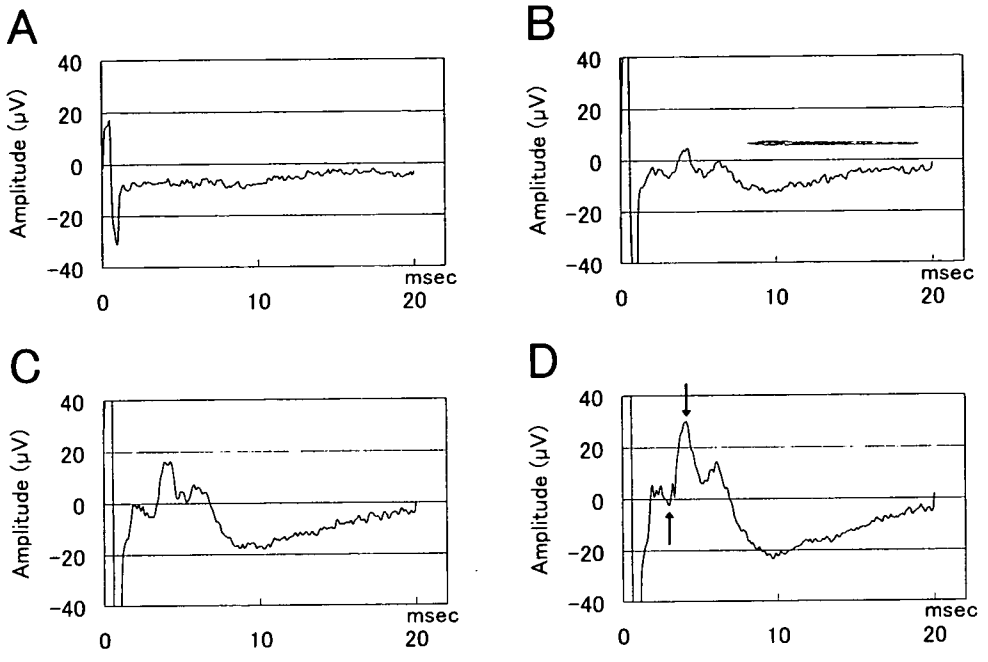

FIGURE 9. Example of EP recorded in optic chiasma in response to STS with currents of 60 μA (A), 150 μA (B), 300 μA (C), and 500 μA (D) in cat 7. (D) *Arrows*: first negative peak and second positive peak. EP amplitude was evaluated between these peaks.

retina. To confirm that our system measured the retinal area in which the retina was activated, we examined whether the reflectance of infrared light changed in response to flickering visible light stimulation. Our results showed that a decrease in reflectance in the area corresponded with the light-stimulated striped area (Fig. 3), as reported by Ts'o et al. for light stimulation (Ts'o D, et al. *IOVS* 2004;45:ARVO E-Abstract 3495). Tsunoda et al.[8] also reported decreased light reflectance that peaked within 1 second of light stimulation, faster than our observation (peak approximately 7 seconds; Fig. 3). This discrepancy might have occurred because we used continuous flickering light whereas Tsunoda et al.[8] used single-flashed light. Indeed, the time course of the reflectance change in our case was similar to that of Ts'o D, et al. (*IOVS* 2004;45:ARVO E-abstract 3495) who used flickering light.

With focal electrical stimulation, the reflectance increased or decreased depending on the retinal area (Fig. 4). Reflectance changes induced by electrical stimulation had fast and slow phases, whereas those induced by light stimulation were monotonic, suggesting that the time course to activate the retina that induced the reflectance changes was different by light stimulation than it was by electrical stimulation (Figs. 3–6).

The origin of the positive change of reflection is a matter of discussion, but, because the time course of positive and negative reflection changes were similar, we suggest that both positive and negative reflection changes were evoked by the same mechanism related to the retinal activation (Figs. 5, 6). Therefore, we added the absolute value of positive and negative reflectance change as a parameter of reflectance changes.

The change in reflectance intensity was linearly related to the intensity of the electrical current (Fig. 6). If we consider that the change in reflectance was correlated with the local retinal response,[8] the value of the reflectance change might have reflected the degree of retinal activation induced by the electrical current. The area of the reflectance change was correlated with the simulating current, suggesting that the area of reflectance change represented the area of the retina activated by electrical stimulation (Fig. 8). This supports the results of electrophysiological studies showing that the area of retinal excitation was correlated with the intensity of electrical current (Kanda H, et al. *IOVS* 2005;46:ARVO E-Abstract 1499).

In the electrophysiological data from the OX, the maximum amplitude of the EP was strongly correlated with the intensity of stimulus current (Fig. 10), suggesting that focal electrical stimulation in the retina activated retinal ganglion cells (RGCs) in proportion to the intensity of stimulation current. EP amplitude was correlated with the total pixels of reflectance change in the retina, suggesting that the area of reflectance change represented neuronal changes in the retina, which led to the excitation of the RGCs.

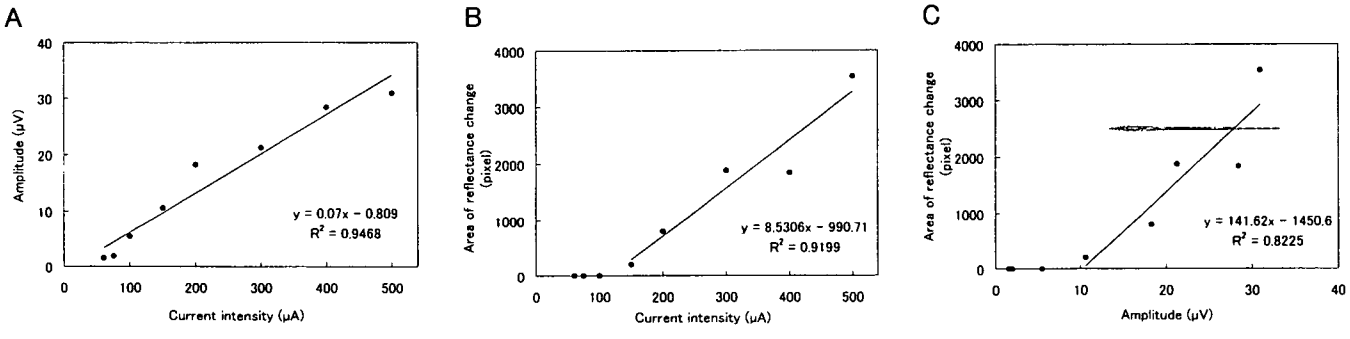

FIGURE 10. Relationships between EP amplitude and stimulus intensity (A), area and stimulus intensity (B), and area and EP amplitude in cat 7 (C).

The threshold current of retinal activation was different for each cat. The reason for this might have been related to the degree of electrode connection to the sclera, which could have been different in each cat. Because the area of reflectance change was correlated with the stimulating current, we may apply this optical imaging system to the artificial retina in humans.

The area of reflectance change is confined to the area around the stimulating electrode with threshold currents (Fig. 7A). Thus, the resolution of the electrode and the optimum parameter for the stimulation of each electrode can be determined objectively.

References

1. Ts'o DY, Frostig RD, Lieke EE, Grinvald A. Functional organization of primate visual cortex revealed by high resolution optical imaging. *Science*. 1990;249:417-420.
2. Frostig RD, Lieke EE, Ts'o DY, Grinvald A. Cortical functional architecture and local coupling between neuronal activity and the microcirculation revealed by in vivo high-resolution optical imaging of intrinsic signals. *Proc Natl Acad Sci USA*. 1990;87:6082-6086.
3. Tsunoda K, Yamane Y, Nishizaki M, Tanifuji M. Complex objects are represented in macaque inferotemporal cortex by the combination of feature columns. *Nat Neurosci*. 2001;4:832-838.
4. Taga G, Asakawa K, Maki A, Konishi Y, Koizumi H. Brain imaging in awake infants by near-infrared optical tomography. *Proc Natl Acad Sci USA*. 2003;100:10722-70727.
5. Das A, Gilbert CD. Long-range horizontal connections and their role in cortical reorganization revealed by optical recording of cat primary-visual-cortex. *Nature*. 1995;375:780-784.
6. Cohen LB. Changes in neuron structure during action potential propagation and synaptic transmission. *Physiol Rev*. 1973;53:373-418.
7. Holthoff K, Writte OW. Intrinsic optical signals in rat neocortical slices measured with near-infrared dark-field microscopy reveal changes in extracellular space. *J Neurosci*. 1996;16:2740-2749.
8. Tsunoda K, Oguchi Y, Hanazono G, Tanifuji M. Mapping cone- and rod- induced retinal responsiveness in macaque retina by optical imaging. *Invest Ophthalmol Vis Sci*. 2004;45:3820-3826.
9. Riva CE, Logean E, Falsini B. Visually evoked hemodynamical response and assessment of neurovascular coupling in the optic nerve and retina. *Prog Retin Eye Res*. 2005;24:183-215.
10. Abramoff MD, Kwon YH, Ts'o D, et al. Visual stimulus-induced changes in human near-infrared fundus reflectance. *Invest Ophthalmol Vis Sci*. 2006;47:715-721.
11. Sutter EE, Tran D. The field topography of ERG components in man, I: the photopic luminance response. *Vision Res*. 1992;32:433-446.
12. Zrenner E. Will retinal implants restore vision? *Science*. 2002;295:1022-1025.
13. Humayun MS, Weiland JD, Fujii GY, et al. Visual perception in a blind subject with a chronic microelectronic retinal prosthesis. *Vision Res*. 2003;43:2573-2581.
14. Chow AY, Chow VY, Packo KH, Pollack JS, Peyman GA, Schuchard R. The artificial silicon retina microchip for the treatment of vision loss from retinitis pigmentosa. *Arch Ophthalmol*. 2004;122:460-469.
15. Rizzo JF 3rd, Wyatt J, Loewenstein J, Kelly S, Shire D. Perceptual efficacy of electrical stimulation of human retina with a microelectrode array during short-term surgical trials. *Invest Ophthalmol Vis Sci*. 2003;44:5362-5369.
16. Kanda H, Morimoto T, Fujikado T, Tano Y, Fukuda Y, Sawai H. Electrophysiological studies on the feasibility of suprachoroidal-transretinal stimulation for artificial vision in normal and RCS Rat. *Invest Ophthalmol Vis Sci*. 2004;45:560-566.
17. Eckhorn R, Wilms M, Schanze T, et al. Visual resolution with retinal implants estimated from recordings in cat visual cortex. *Vision Res*. 2006;46:2675-2690.

Correlation between Focal Macular Electroretinograms and Angiographic Findings after Photodynamic Therapy

Kohei Ishikawa, Mineo Kondo, Yasuki Ito, Masato Kikuchi, Hiroaki Nishihara, Chang-Hua Piao, Tadasu Sugita, and Hiroko Terasaki

Purpose. It is known that the amplitudes of the multifocal electroretinograms are generally reduced soon after photodynamic therapy (PDT). The purpose of this study was to determine whether this amplitude reduction correlates with the changes in macular thickness or with changes in choroidal circulation.

Methods. Thirty-seven eyes that were successfully treated by PDT were studied. Focal macular electroretinograms (fmERGs) and optical coherence tomography were performed before and 1 week, 1 month, and 3 months after PDT. Indocyanine green angiography was performed before and 3 months after PDT. The indocyanine green angiographic findings were classified into two groups: group A, with indistinct hypofluorescence at the site of the PDT, and group B, with well-defined hypofluorescence borders coinciding with the site of the PDT.

Results. The mean amplitudes of the fmERGs were significantly reduced at 1 week after PDT ($P < 0.05$). The correlations between the changes in the amplitude of the fmERG and the changes in macular thickness were not significant. Sixteen (43%) of the study eyes were classified into group A and 21 (57%) into group B by indocyanine green angiography. The mean ratio of the fmERG b-wave 1 week after PDT to that before PDT was 1.14 ± 0.62 in group A and 0.65 ± 0.29 in group B. This difference was statistically significant ($P < 0.01$).

Conclusions. One of the possibilities that could explain the reduction in the amplitude of the fmERGs soon after PDT is the reduction in choroidal circulation caused by the PDT. (*Invest Ophthalmol Vis Sci.* 2007;48:2254-2259) DOI:10.1167/iovs.06-1277

Photodynamic therapy (PDT) with verteporfin is one option for the management of choroidal neovascularization (CNV) associated with age-related macular degeneration (AMD) and other retinal diseases.[1-6] In this treatment, a nonthermal laser beam is applied focally to the CNV lesion after intravenous injection of a photosensitizer (verteporfin), and the energy from the laser beam is preferentially absorbed and retained in the neovascular tissue. Photosensitizers activated by the laser produce photochemical reactions that lead to thrombosis of the vessels within the CNV. Randomized clinical trials have shown that PDT with verteporfin can significantly reduce the rate of moderate and severe visual decrease in patients with AMD and myopic CNV.[1-4]

Although PDT has been generally regarded as a safe procedure, acute visual disturbances have been reported in a small number of cases relatively early after PDT. For example, in the VIP study,[4] 10 (4.4%) of 225 patients reported a severe visual decrease within 7 days after PDT, and 3 (0.7%) of 402 patients had a similar decrease in the TAP study.[2] A review of these cases[7] showed that the acute visual loss after PDT was associated with abnormal findings including serous retinal detachment, subretinal hemorrhage, abnormal choroidal perfusion, and retinal color changes. However, four of these patients did not show any abnormality by ophthalmoscopy and fluorescein angiography.

To study the changes in macular function after PDT objectively, multifocal electroretinograms (mfERGs) have been recorded by many researchers before and after PDT.[8-13] In some of these studies,[9,10,12] it was reported that the amplitudes of mfERGs were reduced within 2 weeks after PDT and then recovered gradually over 3 months. These results suggest that macular function may be transiently impaired after PDT. However, the exact mechanism causing the retinal dysfunction has not been determined, although several possibilities have been proposed: ischemic changes induced by altered choroidal circulation,[12,14] acute inflammatory response associated with vascular leakage,[12,14] and damage to the photoreceptors or bipolar cells by the PDT.[13]

The purpose of this study was to determine the cause of depressed retinal function that occurs soon after PDT. To answer this question, we examined macular thickness by optical coherence tomography (OCT) and choroidal circulation by indocyanine green angiography (ICGA) and compared them to the focal macular electroretinograms (fmERGs). The reduction in the amplitude of the fmERGs after PDT was significantly greater in patients with a well-defined choroidal hypofluorescence border coinciding with the site of the PDT than in patients with indistinct choroidal hypofluorescence. This suggests that the transient amplitude decrease in fmERGs after PDT is probably related to the decreased choroidal circulation caused by PDT.

Methods

Patients

The medical records of 37 eyes of 36 patients (25 men, 11 women, mean age 72.2 ± 8.7 years, mean ± SD), who underwent PDT at the Nagoya University Hospital, were examined, retrospectively. Patients with subfoveal CNV caused by AMD and those with polypoidal choroidal vasculopathy (PCV) were studied. Patients who had CNV lesions that were due to other retinal diseases or who had other ophthalmic diseases were excluded. Of the 37 eyes, 22 (59%) had AMD and 15 (41%) had PCV. We measured the greatest linear dimension (GLD) before PDT by fluorescein angiography, according to the guidelines of the TAP (Treatment of Age-Related Macular Degeneration with Photo-

From the Department of Ophthalmology, Nagoya University Graduate School of Medicine, Nagoya, Japan.

Supported by Grants-in-Aid 18791272 (KI), 18597913 (MK), 16390497 (HT), and 18390466 (HT) from the Japanese Ministry of Education, Science, Sports and Culture.

Submitted for publication October 24, 2006; revised December 27, 2006; accepted February 5, 2007.

Disclosure: **K. Ishikawa**, None; **M. Kondo**, None; **Y. Ito**, None; **M. Kikuchi**, None; **H. Nishihara**, None; **C.-H. Piao**, None; **T. Sugita**, None; **H. Terasaki**, None

The publication costs of this article were defrayed in part by page charge payment. This article must therefore be marked "*advertisement*" in accordance with 18 U.S.C. §1734 solely to indicate this fact.

Corresponding author: Kohei Ishikawa, Department of Ophthalmology, Nagoya University Graduate School of Medicine, 65 Tsurumacho, Showa-ku, Nagoya 466-8550, Japan; kohei@med.nagoya-u.ac.jp.

dynamic Therapy)[1,2] and VIP (Verteporfin in Photodynamic Therapy Study)[3,4] studies. The mean of the GLD of the lesion was 3621 ± 1320 μm (± SD; range, 1676–6479).

The research was conducted in accordance with the institutional guidelines of Nagoya University, and the procedures used conformed to the tenets of the World Medical Association's Declaration of Helsinki. An informed consent had been obtained for the examinations and PDT from each of the patients after they were provided sufficient information on the procedures to be used.

Visual Acuity

The standard Japanese chart was used to measure visual acuity, and the results were converted to Snellen visual acuity and to the logarithm of the minimal angle of resolution (logMAR) for statistical analyses.

Photodynamic Therapy

PDT was performed according to the guidelines of the TAP[1,2] and VIP[3,4] studies. Patients received 6 mg/m^2 intravenous verteporfin (Visudyne; Novartis, Basel, Switzerland) over a 10-minute period. Fifteen minutes after the beginning of the infusion, a 689-nm diode laser was used to deliver 600 mW/cm^2 for at least 83 seconds, to produce an energy dose of 50 J/cm^2. The diameter of the laser spot was calculated to be 1000 μm larger than the GLD of the CNV lesion. After treatment, patients were given protective spectacles, and they were instructed to avoid direct sunlight or strong light for 3 days.

Focal Macular Electroretinograms

fmERGs were recorded before, and 1 week, 1 month, and 3 months after PDT. Our system for eliciting and recording fmERGs has been described in detail.[15,16] Briefly, an infrared fundus camera, equipped with a stimulus light, background illumination, and fixation target, was used. The image from the camera was fed to a television monitor, and the examiner used the images on the monitor to maintain the stimulus centered on the fovea.

The size of the stimulus spot was 15°, and the background light was delivered to the eye from the fundus camera at a visual angle of 45°. Additional background illumination outside the central 45° produced a homogeneous background for nearly the entire visual field. The luminances of the white stimulus light and background light were 29.46 and 2.89 cd/m^2, respectively. These luminances were measured at the corneal surface and then converted to the retinal surface.

A Burian-Allen bipolar contact lens electrode was used to pick-up the fmERGs. This contact lens electrode system allowed not only low electrical noise but also permitted a clear view of the fundus by the camera during the recordings.

After the patients' pupils were fully dilated with 0.5% tropicamide and 0.5% phenylephrine hydrochloride, fmERGs were elicited by 5 Hz rectangular stimuli (100-ms light on and 100-ms light off). A total of 512 responses were averaged by a signal processor. A time constant of 0.03 seconds with a 100-Hz high-cut filter on the amplifier was used to record the a- and b-waves.

The amplitude of the a-wave was measured from the baseline to the first negative trough, and the amplitude of b-wave was measured from the trough of the a-wave to the positive peak of the b-wave. The noise level of our recording system was <0.4 μV.

Macular Thickness Measured by OCT

The macular thickness was measured by OCT (Stratus OCT; Carl Zeiss Meditec, Dublin, CA) before, and 1 week, 1 month, and 3 months after PDT. Six radial scans of 6-mm length were made by using the Fast Macular Thickness Map (FMTM) protocol. Because the FMTM system often misreads the exact borders of the retina in the presence of a CNV, the thickness of the retina was determined by our new program (Ishikawa K et al. *IOVS* 2005;46:ARVO E-Abstract 1550). For this program, the user is able to set eight or more cursors above and below a selected area manually, and for this study, the upper cursors were set on the internal limiting membrane (ILM), and the lower cursors were set on the retinal pigment epithelium (RPE) side of the retina. Another set of cursors was set at the fovea of the OCT images. When a CNV extended above the RPE, the lower-cursors were set on the retinal side of the CNV contour. The program then automatically calculated the average macular thickness within a 3-mm (diameter) circle centered at the fovea.

Indocyanine Green Angiography

ICGA was performed with a confocal scanning laser ophthalmoscope (Heidelberg Retina Angiography II; Heidelberg Engineering, Dossenheim, Germany) before and 3 months after PDT. All eyes were classified into two groups from the ICGA findings at 10 minutes: group A included eyes with indistinct hypofluorescence at the site of the PDT, and group B included eyes with a well-defined hypofluorescence border coinciding with the site of the PDT. Eyes in which the border of the hypofluorescent area could be clearly recognized for 360° were defined as having well-defined hypofluorescence borders. This classification was performed by two retinal specialists (MK, HN) who were masked to the clinical information of the patients.

Statistical Analyses

The visual acuity, macular thickness, amplitudes, and implicit times of fmERGs after PDT were compared with the corresponding values recorded before by the nonparametric Wilcoxon signed rank test. The Mann-Whitney *U* test was used to compare two groups, and the Pearson's correlation coefficient and the Fisher *r*-to-*z* test for analysis of correlation. The data were analyzed with commercial software (Stat-

TABLE 1. fmERGs before and 1 Week, 1 Month, and 3 Months after PDT

	Pre-PDT	Post-1 W	Post-1 M	Post-3 M	Normal Subjects (n = 112)
Visual acuity (logMAR)	0.71 ± 0.32	0.63 ± 0.35	0.63 ± 0.36	0.65 ± 0.42	
P*		**0.0068**	**0.0241**	0.1232	
Amplitide (μV)					
a-wave	0.52 ± 0.53	0.36 ± 0.45	0.45 ± 0.41	0.47 ± 0.48	2.10 ± 0.64
P*		**0.0226**	0.33	0.3873	
b-wave	1.92 ± 0.91	1.46 ± 0.72	1.49 ± 0.58	1.79 ± 0.67	4.89 ± 0.94
P*		**0.0006**	**0.0009**	0.1255	
Implicit time (ms)					
a-wave	25.8 ± 3.3	27.2 ± 4.5	25.8 ± 3.8	25.2 ± 4.0	21.9 ± 1.7
P*		0.12	0.9158	0.2353	
b-wave	57.0 ± 10.2	56.8 ± 9.2	54.9 ± 9.5	55.3 ± 8.9	42.8 ± 2.1
P*		0.5932	0.1114	0.2449	

Data are the mean ± SD.

* Wilcoxon signed-rank test (compared with before PDT). Significant differences are in bold.

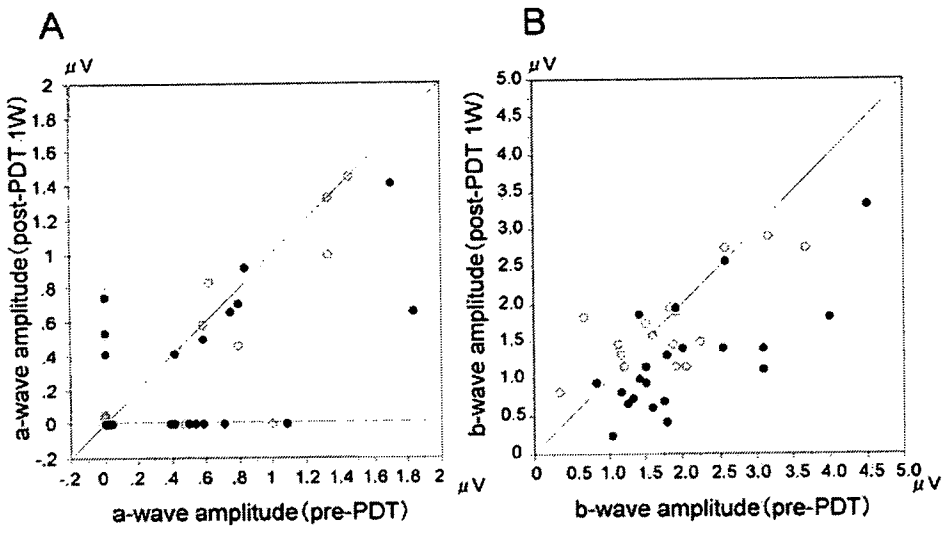

FIGURE 1. Comparison of the a- and b-waves of the fmERGs before and after PDT. (○) Eyes with an indistinct hypofluorescence at the site of the PDT (group A); (●) eyes with a well-defined hypofluorescence border coinciding with the site of the PDT (group B). (A) Amplitude of the a-wave of fmERG before (abscissa) and 1 week after (ordinate) PDT. (B) Amplitude of the b-wave before (abscissa) and 1 week after (ordinate) PDT.

View ver. 5; SAS Institute, Cary, NC). $P < 0.05$ was considered to be statistically significant.

RESULTS

Visual Acuity

The mean best corrected visual acuity (BCVA) in logMAR units was 0.71 ± 0.32 (mean ± SD; 20/103, Snellen equivalent) before PDT, and it improved to 0.63 ± 0.35 (20/85) 1 week after PDT. The BCVA then stabilized at 0.63 ± 0.36 (20/85) and 0.65 ± 0.42 (20/89) at 1 and 3 months, respectively, after PDT. The BCVA at 1 week and 1 month was significantly better than that before PDT ($P < 0.01$ at 1week; $P < 0.05$ at 1 month, Wilcoxon signed-rank test, Table 1).

For this study, an increase of >0.2 logMAR was defined as an improvement, and a decrease of >0.2 logMAR was defined as a worsening. A change in the BCVA of < ±0.2 logMAR was classified as unchanged BCVA. At 1 week after PDT, 29 (78%) eyes were unchanged, 8 (22%) had an improvement, and none had a decrease. At 3 months after PDT, 23 (62%) were unchanged, 10 (27%) had an improvement, and 4 (11%) had a decrease.

Focal Macular Electroretinograms

The mean amplitude of the b-wave was reduced to 76% and 78% of the pre-PDT amplitude at 1 week and 1 month after PDT, respectively. The b-waves then recovered to 93% at 3 months after PDT (Table 1). The reductions in the b-wave amplitude at 1 week and 1 month after PDT were statistically significant ($P < 0.001$, Wilcoxon signed rank test).

Similarly, the amplitude of the a-wave was reduced to 59% of the pre-PDT value, and then gradually increased to 87% and 90% of the pre-PDT level at 1 and 3 months after PDT, respectively (Table 1). The reduction in amplitude at 1 week after PDT was statistically significant ($P = 0.02$).

There were no significant changes in the implicit times of the a- and b-waves within 3 months after PDT (Table 1).

A comparison of the amplitudes of the a- and b-waves of the fmERGs before (abscissa) and 1 week after (ordinate) PDT for the 37 eyes is shown in Figure 1. The amplitude of the a-wave was decreased in 16 of 37 eyes at 1 week after PDT. In 12 of 37 eyes, the amplitude of the a-wave was nonrecordable before and 1 week after PDT. The b-wave amplitude was decreased in 23 of 37 eyes at 1 week after PDT.

Macular Thickness

The macular thicknesses within a 3-mm-diameter circle before and 1 week after PDT in all 37 eyes are plotted in Figure 2. The macular thickness tended to be reduced slightly after PDT, but this reduction was not statistically significant (i.e., before PDT, the thickness was 338.9 ± 68.0 μm; and 1 week after PDT, it was 322.1 ± 83.5 μm; $P = 0.06$, Wilcoxon signed-rank test).

Next, we investigated whether the reduced fmERG seen 1 week after PDT was related to the changes in macular thickness at 1 week after PDT. The relative changes in the b-wave amplitude at 1 week after PDT were not significantly correlated with the relative changes in the macular thickness at 1 week after PDT ($r = 0.197$, Pearson's correlation coefficient, $P = 0.2436$, Fisher r to z).

ICGA Findings

Finally, we studied the ICGA findings in 37 eyes at 3 months after PDT. We found that 16 (43%) eyes showed an indistinct

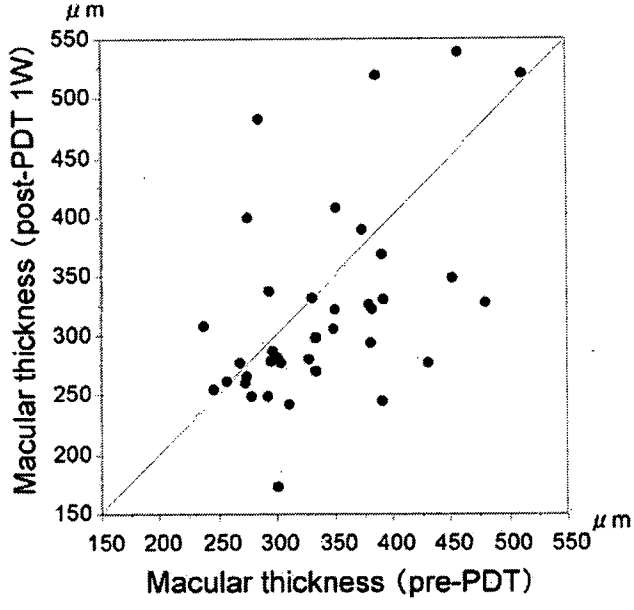

FIGURE 2. Macular thickness measured by the OCT before (abscissa) and 1 week after (ordinate) PDT.

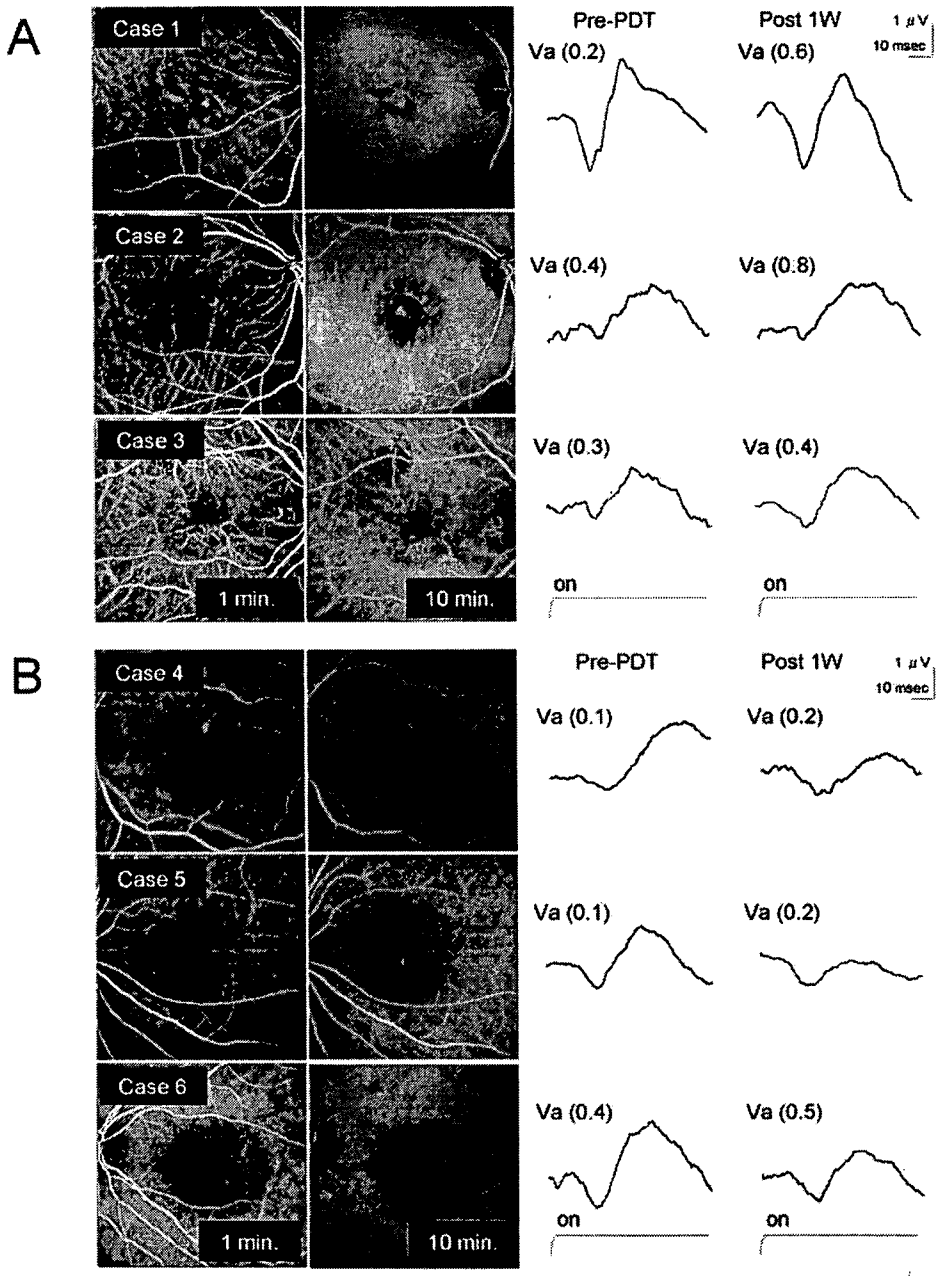

FIGURE 3. Representative ICGA findings at 3 months after photodynamic therapy and focal macular electroretinograms waveforms before and 1 week after photodynamic therapy. (A) Three cases from group A: eyes with no or indistinct hypofluorescence at the site of the PDT. (B) Three cases from group B: eyes with well-defined hypofluorescence borders coinciding with the site of the PDT.

hypofluorescence at the site of the PDT (group A), and 21 (57%) eyes showed a well-defined hypofluorescence border coinciding with the site of the PDT (group B). Representative ICGA at 1 and 10 minutes after infusion and the fmERGs for groups A and B are shown in Figures 3A and 3B. The clinical characteristics of the two groups are summarized in Table 2.

We examined whether there was any difference in the relative amplitudes of the fmERGs after PDT between the two groups and found that the relative b-wave amplitude at 1 week after PDT to that before PDT was significantly larger in group A (1.14 ± 0.62) than that in group B (0.65 ± 0.29; $P = 0.0015$, Mann-Whitney U test, Fig. 4A). This difference was still significant at 1 month after PDT ($P = 0.03$, Fig. 4B), but was not significant at 3 months afterward ($P = 0.13$).

We also investigated whether there was any difference in the macular thickness at 1 week after PDT between these two groups. There was no significant difference in the relative changes in the macular thickness at 1 week after PDT between groups A (0.92 ± 0.20) and B (1.00 ± 0.25, $P = 0.09$).

DISCUSSION

Our results demonstrated that the amplitudes of the fmERGs were transiently reduced after PDT, even though the visual acuity improved after treatment. Thus, at 1 week after PDT, the amplitudes of the a- and b-waves were reduced to 69% and 76% of the pre-PDT values, respectively, but they recovered to the pre-PDT level within 3 months. These changes in the fmERGs after PDT were similar to the results of some previous studies using mfERGs.[9,10,12] For example, Lai et al.[12] reported that the amplitudes of the mfERGs were reduced to 84% to 87% within 2 weeks after PDT, then recovered to the pre-PDT level at 1 month. Therefore, our results support the idea that the macular

TABLE 2. Data for Study Groups before PDT

	Group A	Group B
Eyes (*n*)	16 eyes	21 eyes
Gender		
Male	12	14
Female	4	7
Age (y)	67.2 ± 8.7	75.9 ± 6.8
Visual acuity (logMAR)	0.81 ± 0.30	0.64 ± 0.32
GLD (μm)	2901 ± 1060	4170 ± 1249

Data are expressed as the mean ± SD. Group A: eyes with no or indistinct hypofluorescence at the site of the PDT; group B: eyes with well-defined hypofluorescence borders coinciding with the site of the PDT.

function may be decreased transiently at relatively early stages after PDT.

The exact mechanism of this transient reduction of the macular ERGs after PDT has not been determined and is still controversial.[9,10,12,13] We had hypothesized that the transient reduction of fmERG might be related to morphologic changes at early stages after PDT, because it has been reported that vascular leakage and/or subretinal fluid were transiently increased at the early stages after PDT in clinical[18-20] and animal studies.[21-25] To examine whether these morphologic changes in the macula were related to the reduction of the amplitude of fmERG, we measured the macular thickness (distance from the ILM to the RPE, including subretinal fluid) using the Stratus OCT (Carl Zeiss Meditec, GmbH) and our program (Ishikawa K et al. *IOVS* 2005;46:ARVO E-Abstract 1550). However, we could not find any significant correlation between the changes in the macular thickness and reduction of the fmERGs.

We next hypothesized that the transient amplitude reduction of fmERGs is related to the decrease in choroidal circulation after PDT and examined the ICGA findings. We found that the amplitude reduction of fmERG after PDT was more severe in patients who had a well-defined choroidal hypofluorescence at the site of PDT than in patients with indistinct hypofluorescence of ICGA at 1 week after PDT (Fig. 4A). This difference remained significant at 1 month after PDT (Fig. 4B). These results suggest that the transient amplitude reduction of fmERG after PDT is related to a dysfunction of the outer retina due to the reduced choroidal circulation caused by the PDT.

It is widely accepted that PDT is not perfectly selective for CNV, but can cause partial occlusion of the choroidal vessels. Choroidal hypoperfusion coinciding with the PDT site has been reported in clinical studies.[18,19,26-29] In addition, animal studies have demonstrated that PDT can cause the occlusion of normal choriocapillaris, even though the occlusion is reversible.[21-24] Recently, Tzekov et al.[25] recorded mfERGs and ICGA in two cynomolgus monkeys, and reported that the amplitudes of the mfERGs were reduced to approximately 20% of the pre-PDT level within 1 week after PDT. They suggested that this reduction is due to reduced oxygen supply from the choroid to the outer retina caused by extensive closure of the choroidal vessels after PDT. Our clinical study supports this suggestion.

We also noted that after PDT, the amplitude reduction of the b-wave was more prolonged than that of the a-wave (Table 1). We could not determine the exact reason for this prolonged depression of the b-wave. One possibility is that the middle retinal layer, which is the origin of the b-wave, is also impaired after PDT, and that the functional recovery of middle retinal layer is more delayed than that of the outer retina. We have experienced similar phenomenon in patients with central serous chorioretinopathy.[17]

There were some limitations to our study. First, we recorded ICGA before PDT and 3 months after PDT and did not examine the changes in the choroidal circulation at the early stages after PDT. Therefore, we could not determine whether a correlation exists between the fmERGs and ICGA findings at 1 week and 1 month after PDT. Second, we did not examine the morphologic findings by OCT at the very early stages after PDT (e.g., within 2 to 3 days after PDT). There is recent evidence that acute inflammatory changes after PDT are seen most clearly within 2 to 3 days after PDT.[18-20] Such very early morphologic changes may be related to our fmERG findings. Third, the interpretation for the changes in the macular thickness after PDT is very complex. On the one hand, if there is retinal edema before PDT and if PDT is successful, then the macular thickness may be reduced after PDT, and this thinning may be associated with visual improvement. On the other hand, if PDT damages choroidal blood flow profoundly, then post-PDT macular thinning might be associated with impaired vision and ERG changes.

Finally, we could not determine which factors of the patients contributed to the relatively severe reduction of choroidal circulation after PDT. As shown in Table 2, patients who were older, had larger lesions, and were female tended to have a relatively greater reduction of choroidal circulation after PDT

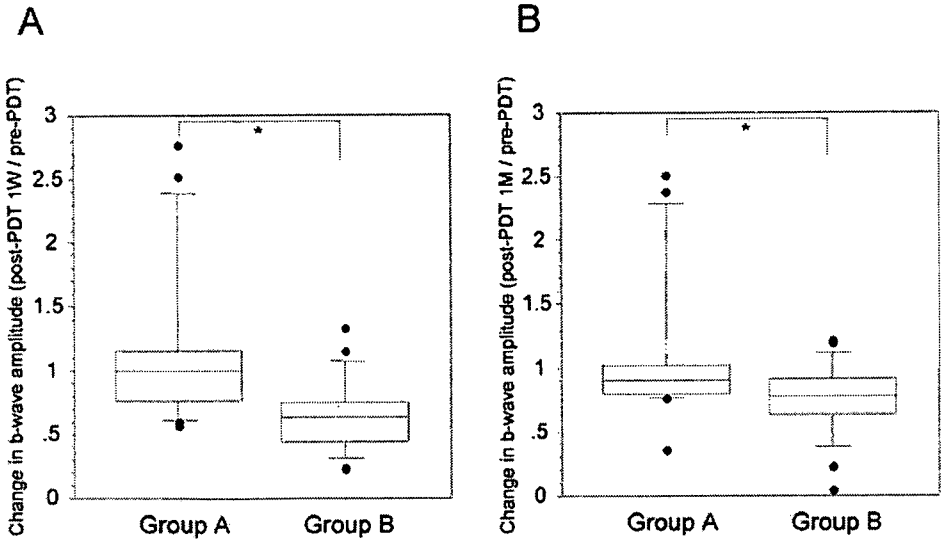

FIGURE 4. (A) Box plots of the relative b-wave amplitudes at 1 week after PDT to that before PDT in groups A and B. (B) Box plots of the relative b-wave amplitudes at 1 month after PDT to that before PDT for the two groups. *Line* within the box indicates the median, the box limits are the 25th and 75th percentiles, the error bars are the 10th and 90th percentiles. There were significant differences between the two groups both 1 week and 1 month after PDT. ($P < 0.05$, Mann-Whitney *U* test).

(group B). However, we are hesitant to conclude that these factors are really involved, because the number of patients was small. Further studies are needed to clarify what factors in the patients are related to the most important effect on choroidal circulation after PDT treatment.

References

1. Treatment of Age-Related Macular Degeneration with Photodynamic Therapy (TAP) Study Group. Photodynamic therapy of subfoveal choroidal neovascularization in age-related macular degeneration with verteporfin: one-year results of 2 randomized clinical trials-TAP report 1. *Arch Ophthalmol.* 1999;117:1329-1345.
2. Treatment of Age-Related Macular Degeneration with Photodynamic Therapy (TAP) Study Group. Photodynamic therapy of subfoveal choroidal neovascularization in age-related macular degeneration with verteporfin: two-year results of two randomized clinical trials-TAP report 2. *Arch Ophthalmol.* 2001;119:198-207.
3. Verteporfin in Photodynamic Therapy Study Group. Photodynamic therapy of subfoveal choroidal neovascularization in pathologic myopia with verteporfin: 1-year results of a randomized clinical trial. VIP report 1. *Ophthalmology.* 2001;108:841-852.
4. Verteporfin in Photodynamic Therapy Study Group. Verteporfin therapy of subfoveal choroidal neovascularization in age-related macular degeneration: two-year results of a randomized clinical trial including lesions with occult with no classic choroidal neovascularization: verteporfin in photodynamic therapy report 2. *Am J Ophthalmol.* 2001;131:541-560.
5. Japanese Age-Related Macular Degeneration Tial (JAT) Study Group. Japanese age-related macular degeneration trial: 1-year results of photodynamic therapy with verteporfin in Japanese patients with subfoveal choroidal neovascularization secondary to age-related macular degeneration. *Am J Ophthalmol.* 2003;136:1049-1061.
6. Verteporfin Roundtable Participants. Guidelines for using verteporfin (Visudyne) in photodynamic therapy for choroidal neovascularization due to age-related macular degeneration and other causes: update. *Retina.* 2005;25:119-134.
7. Treatment of Age-Related Macular Degeneration with Photodynamic Therapy Study Group; Verteporfin in Photodynamic Therapy Study Group. Acute severe visual acuity decrease after photodynamic therapy with verteporfin: case reports from randomized clinical trials-TAP and VIP report no. 3. *Am J Ophthalmol.* 2004;137:683-696.
8. Palmowski AM, Allgayer R, Heinemann-Vernaleken B, Ruprecht KW. Influence of photodynamic therapy in choroidal neovascularization on focal retinal function assessed with the multifocal electroretinogram and perimetry. *Ophthalmology.* 2002;109:1788-1792.
9. Moschos MN, Panayotidis D, Moschos MM, Bouros C, Theodossiadis PG, Theodossiadis GP. A preliminary assessment of macular function by MF-ERG in myopic eyes with CNV with complete response to photodynamic therapy. *Eur J Ophthalmol.* 2003;13:461-467.
10. Rüther K, Breidenbach K, Schwartz R, Hassenstein A, Richard G. Testing central retinal function with multifocal electroretinography before and after photodynamic therapy. *Ophthalmologe.* 2003;100:459-464.
11. Jiang L, Jin C, Wen F, Huang S, Wu D, Wu L. The changes of multifocal electroretinography in the early stage of photodynamic therapy for choroidal neovascularization. *Doc Ophthalmol.* 2003;107:165-170.
12. Lai TY, Chan WM, Lam DS. Transient reduction in retinal function revealed by multifocal electroretinogram after photodynamic therapy. *Am J Ophthalmol.* 2004;137:826-833.
13. Moschos MM, Panayotidis D, Theodossiadis G, Moschos M. Assessment of macular function by multifocal electroretinogram in age-related macular degeneration before and after photodynamic therapy. *J Fr Ophtalmol.* 2004;27:1001-1006.
14. Mennel S, Meyer CH. Transient visual disturbance after photodynamic therapy. *Am J Ophthalmol.* 2005;139:748-749.
15. Miyake Y, Shiroyama N, Ota I, Horiguchi M. Oscillatory potentials in electroretinograms of the human macular region. *Invest Ophthalmol Vis Sci.* 1988;29:1631-1635.
16. Miyake Y. Studies of local macular ERG. *Acta Soc Ophthalmol Jpn.* 1988;92:1418-1449.
17. Miyake Y, Shiroyama N, Ota I, Horiguchi M. Local macular electroretinographic responses in idiopathic central serous chorioretinopathy. *Am J Ophthalmol.* 1988;106:546-550.
18. Costa RA, Farah ME, Cardillo JA, Calucci D, Williams GA. Immediate indocyanine green angiography and optical coherence tomography evaluation after photodynamic therapy for subfoveal choroidal neovascularization. *Retina.* 2003;23:159-165.
19. Michels S, Schmidt-Erfurth U. Sequence of early vascular events after photodynamic therapy. *Invest Ophthalmol Vis Sci.* 2003;44:2147-2154.
20. Rogers AH, Martidis A, Greenberg PB, Puliafito CA. Optical coherence tomography findings following photodynamic therapy of choroidal neovascularization. *Am J Ophthalmol.* 2002;134:566-576.
21. Miller JW, Walsh AW, Kramer M, et al. Photodynamic therapy of experimental choroidal neovascularization using lipoprotein-delivered benzoporphyrin. *Arch Ophthalmol.* 1995;113:810-818.
22. Kramer M, Miller JW, Michaud N, et al. Liposomal benzoporphyrin derivative verteporfin photodynamic therapy: selective treatment of choroidal neovascularization in monkeys. *Ophthalmology.* 1996;103:427-438.
23. Reinke MH, Canakis C, Husain D, et al. Verteporfin photodynamic therapy retreatment of normal retina and choroid in the cynomolgus monkey. *Ophthalmology.* 1999;106:1915-1923.
24. Husain D, Kramer M, Kenny AG, et al. Effects of photodynamic therapy using verteporfin on experimental choroidal neovascularization and normal retina and choroid up to 7 weeks after treatment. *Invest Ophthalmol Vis Sci.* 1999;40:2322-2331.
25. Tzekov R, Lin T, Zhang KM, et al. Ocular changes after photodynamic therapy. *Invest Ophthalmol Vis Sci.* 2006;47:377-385.
26. Schlotzer-Schrehardt U, Viestenz A, Naumann GO, Laqua H, Michels S, Schmidt-Erfurth U. Dose-related structural effects of photodynamic therapy on choroidal and retinal structures of human eyes. *Graefes Arch Clin Exp Ophthalmol.* 2002;240:748-757.
27. Schmidt-Erfurth U, Michels S, Barbazetto I, Laqua H. Photodynamic effects on choroidal neovascularization and physiological choroid. *Invest Ophthalmol Vis Sci.* 2002;43:830-841.
28. Schmidt-Erfurth UM, Michels S. Changes in confocal indocyanine green angiography through two years after photodynamic therapy with verteporfin. *Ophthalmology.* 2003;110:1306-1314.
29. Schmidt-Erfurth U, Laqua H, Schlotzer-Schrehard U, Viestenz A, Naumann GO. Histopathological changes following photodynamic therapy in human eyes. *Arch Ophthalmol.* 2002;120:835-844.

Preservation of Macular Oscillatory Potentials in Eyes of Patients with Retinitis Pigmentosa and Normal Visual Acuity

Kazuteru Ikenoya, Mineo Kondo, Chang-Hua Piao, Shu Kachi, Yozo Miyake, and Hiroko Terasaki

Purpose. To study the functional changes in the macula of the retina in the early stage of retinitis pigmentosa (RP), by analyzing each component of the focal macular electroretinogram (fmERG).

Methods. fmERGs were recorded from 39 patients with RP with normal visual acuity (>1.0) under direct fundus observation using a modified infrared fundus camera and 5°, 10°, and 15° stimulus spots. The amplitudes and implicit times of the a-wave, b-wave, and oscillatory potentials (OPs) in the patients with RP were compared to those from 30 age-similar normal control subjects.

Results. The amplitudes of the different components of the fmERGs in patients with RP ranged from severely reduced to normal. The degree of amplitude reduction increased as the size of the stimulus spot increased in the patients with RP. The relative amplitudes of the OPs (67% of the mean in normal subjects) were better preserved than that of the b-wave (46%) and the a-wave (39%) in a 10° spot in the patients with RP.

Conclusions. The relative preservation of the OPs in the patients with RP could be due to either the buffering effect of the large receptive fields of the OP generators or to the retinal remodeling after the progressive loss of photoreceptors. Recordings of each component of fmERG can provide important information on the different layers of the central retina in RP eyes and can add to the understanding of the pathophysiology of RP. (*Invest Ophthalmol Vis Sci.* 2007;48:3312-3317) DOI: 10.1167/iovs.06-1417

Retinitis pigmentosa (RP) is a group of inherited retinal degenerations characterized by progressive loss of photoreceptors and eventual widespread atrophy of the retina.[1-4] The initial visual impairment in patients with RP is usually night blindness and visual field loss in the periphery; the central visual function is usually affected at the later stages of the disease. RP is genetically heterogeneous. At present, approximately 40 genes have been identified as causing RP (http://www.sph.uth.tmc.edu/retnet/ provided in the public domain by the University of Texas Houston Health Science Center, Houston, TX).

From the Department of Ophthalmology, Nagoya University Graduate School of Medicine, Nagoya, Japan.

Supported by Grant-in-Aid 18591913 (MK), and 18390466 (HT) from the Ministry of Education, Science, Sports and Culture, Japan.

Submitted for publication November 29, 2006; revised January 9, 2007; accepted April 9, 2007.

Disclosure: **K. Ikenoya**, None; **M. Kondo**, None; **C.-H. Piao**, None; **S. Kachi**, None; **Y. Miyake**, None; **H. Terasaki**, None

The publication costs of this article were defrayed in part by page charge payment. This article must therefore be marked "*advertisement*" in accordance with 18 U.S.C. §1734 solely to indicate this fact.

Corresponding author: Mineo Kondo, Department of Ophthalmology, Nagoya University Graduate School of Medicine, 65 Tsuruma-cho, Showa-ku, Nagoya 466-8550, Japan; kondomi@med.nagoya-u.ac.jp.

Because the central retinal function is relatively better preserved than the peripheral retina until the late stages of RP, it is important to evaluate the functional changes in the macular area of patients with RP, not only for visual prognosis but also for studying the pathophysiology of the disease processes. The full-field electroretinograms (ERGs) have traditionally been used to assess objectively the retinal function of patients with RP. However, the full-field ERG is a mass potential from the entire retina, and it is not known how the local macular function contributes to the full-field ERG. To overcome these problems, focal (f)ERGs[5-9] and multifocal (mf)ERGs[10-17] have been used to assess the macular function of eyes with RP, because these techniques can elicit electrical activities from localized retinal areas. However at present, there are no results on the alterations of the a-wave, b-wave, and oscillatory potentials (OPs) in the maculae of patients with RP.

Thus, the purpose of this study was to determine the functional changes in the different retinal layers of the macular area by analyzing each component of the focal macular (fm)ERGs at a relatively early stage of RP. We wanted to determine whether the amplitudes of OPs are better preserved than those of the a- and b-waves in the maculae of patients with RP. Our results are the first clinical demonstration that neural activities from the inner retina are better preserved than those from the middle and outer retina in the macular area of patients with RP.

Methods

Subjects

We retrospectively reviewed the fmERGs of 127 patients with RP (62 men, 65 women), that were recorded from 1987 to 2006 in the Department of Ophthalmology, Nagoya University Hospital. The clinical diagnosis of RP was based on the funduscopic findings, visual fields, and ISCEV (International Society for Clinical Electrophysiology of Vision) standard full-field ERGs.[18] The inclusion criteria were patients with RP who had received a complete medical examination including best corrected visual acuity, fundus examination, Goldmann kinetic visual field, full-field ERGs, and fmERGs; patients whose best corrected visual acuity was 1.0 or better; patients whose Goldmann kinetic visual fields by the I4e target were of a >5° radius; and those whose amplitude in the fmERG for 15° stimulus spot was detectable (>0.4 μV). We used these inclusion criteria for the definition of early-stage RP, because most patients with RP whose visual acuity is <0.8 or whose Goldmann kinetic visual fields by I4e target were <5° had undetectable fmERGs. Waveform analysis was very difficult or impossible in these patients because of the severely reduced fmERGs.

The exclusion criteria were patients with atypical RP (e.g., central RP, sector RP, or unilateral RP), patients with opacities in the media including cataracts, and patients with cystoid macular edema. If the fmERG were recorded from both eyes with visual acuity of >1.0, the data from the right eye were used for the analyses. The Goldmann kinetic visual fields were determined with the V4e and I4e white test light against the standard white background of 31.5 apostilbs.

Based on the inclusion and exclusion criteria, the fmERGs of 39 eyes of 39 patients with RP (18 men, 21 women; mean age, 37.9 ± 15.4

Investigative Ophthalmology & Visual Science, July 2007, Vol. 48, No. 7